Electrohydrodynamic patterns in macroion dispersions under a strong electric field

H. Isambert,[1,*] A. Ajdari,[1] J-L. Viovy,[2] and J. Prost[2]
[1]*Laboratoire de Physico-Chimie Théorique, URA CNRS 1382, ESPCI, 10 rue Vauquelin, 75231 Paris Cedex 05, France*
[2]*Section de Recherche, Institut Curie, 11 rue Pierre et Marie Curie, 75231 Paris Cedex 05, France*
(Received 15 May 1997)

Recent reports have shown that initially homogeneous solutions of charged colloidal particles or polyelectrolytes may develop instabilities under strong electric field. In particular, striking dynamical structures forming quasi-stationary zigzag patterns have been observed, under strong ac electric field, when these macroion dispersions are confined into a slab cell. We develop in this paper the basis of a theoretical approach aimed at describing the large scale, long time electrokinetic phenomena occurring, under strong electric field, within a dispersion of macroions in a simple electrolyte of high ionic strength. We assume that the macroions' charges can be described, at large length scales, by a smooth charge profile that merely generates some small perturbations on the already out-of-equilibrium situation of a simple electrolyte under strong electric field. This allows us to overcome the complexity of the nonlinear electrokinetic equations by expanding them around the far-from-equilibrium system with no macroion. This approach is therefore to be contrasted with the classical theory for which the perturbations of the ionic concentrations are evaluated as linear responses to a ''weak'' applied electric field with respect to their equilibrium distributions around a macroion at rest. We show here that the out-of-equilibrium ionic distributions in the solution are perturbed over large length scales in the vicinity of the macroions, which leads to the breakdown of (equilibrium) electroneutrality in the solution far beyond the Debye length scales. The electrical body force arising from the coupling between this large scale charge density and the applied electric field eventually triggers some electrohydrodynamic flows which, in turn, convect the very slowly diffusing macroions in the solution. Numerical resolutions of the model in two analytical limit regimes show that this process is able to select quasistationary dynamical patterns from preexisting inhomogeneous distributions of macroions, in good agreement with experimental observations. In addition, we show, using simple dynamical scaling arguments, that this nonlinear coupling between the macroion density fluctuations and the associated electrohydrodynamic flows dominates the large scale, long time stochastic dynamics of the macroion distribution, suggesting that it might also be responsible, through a noise-driven process, for the primary segregation itself. [S1063-651X(97)13710-2]

PACS number(s): 82.70.Dd, 47.54.+r, 82.45.+z, 83.80.Gv

I. INTRODUCTION

The motivation for this work originated from striking observations done by Mitnik and co-workers [1,2] while studying DNA capillary electrophoresis. In principle, the use of microcapillaries, filled with a neutral polymer solution as sieving medium, allows one to apply strong electric fields and, thus, achieve fast electrophoretic separation [3]. However, Mitnik *et al*. discovered that solutions of monodisperse large DNA fragments become inhomogeneous once subjected to an electric field stronger than a few tens of V/cm. This electric-field-induced DNA segregation, occurring even in the presence of neutral polymer chains used as sieving medium, leads to ''artificial'' peaks on electrophoregrams when one attempts to separate DNA fragments longer than a few kilobase pairs. The phenomenon is therefore, to date, a major limitation to this otherwise very promising technique for molecular genetics. The experimental observations become even more puzzling when the DNA solution is confined not in a capillary but between two glass plates, with an ac electric field applied parallel to the plates [2,4]. Striking zigzag patterns form in the confined DNA solution as depicted in Figs. 1 and 2. Interestingly, very similar patterns have also been observed by other groups with quite different charged colloidal systems such as polystyrene spheres [5] or even China clay [6]. This demonstrates that the underlying physics is a very general phenomenon, i.e., independent of the microscopic nature of the colloidal particles or the polyelectrolytes.

We present in this paper our interpretation of the physical origin of the pattern formation in these macroion dispersions under strong electric field. Some of the general ideas founding this analysis have already been outlined [4]. In the remainder of the Introduction we first recall the main experimental features of the observed electric-field-induced patterning of DNA solutions confined in a quasi-two-dimensional (2D) geometry. We then briefly review and discuss the classical theoretical approach to electrophoresis of macroions in electrolyte solutions of high ionic strength, before outlining the general ideas of the theoretical approach we propose in this paper.

Typical experiments are performed in a slab cell filled with 30 μg/ml of λ-DNA labeled with a fluorescent dye (separation between the parallel glass plates is $a \simeq 10$ μm). The λ-DNA is a 16 μm long DNA fragment [48.5 kilobase (kbp)] taking a coil configuration ($R_g \simeq 1$ μm) in the buffer solution used. Each λ-DNA molecule is known to carry

*Present address: Center for Studies in Physics and Biology, The Rockefeller University, Box 25, 1230 York Ave., New York, NY 10021-6399. Electronic address: isambert@eds2.rockefeller.edu

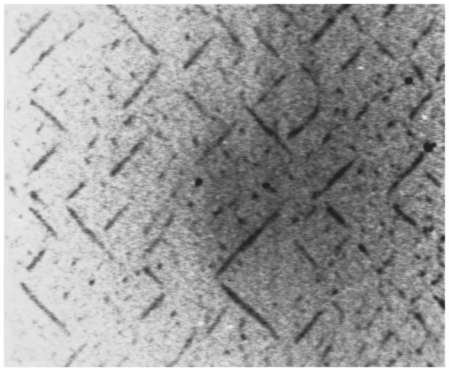

FIG. 1. Top view of the horizontal slab cell containing 30 μg/ml of λ-phage DNA (Appligene, Illkirch, F) in 1X TBE buffer (89 mM Tris-boric acid, 2.5 mM EDTA), containing 10 μM ethidium bromide for fluorescence visualization. A thickness of 10 ± 1 μm is imposed by dispersing in the solution a few latex spheres of diameter 10 μm (Polysciences, Eppelheinm, D). The negative image (covering 300 μm) is taken 2 min after the onset of a 300 V/cm ac field, in the horizontal direction, at the frequency 2 Hz. The angle of tilt between the direction of the electric field and the elongated aggregates is $\theta\simeq\pm45°$ [2].

roughly 50 000 elementary charges [7] that correspond to a mean ''fixed'' charge concentration of about 10^{-3} mol/l in the coil region, 100 times smaller than the ionic strength of the buffer used (see [1] for further experimental details). 0.01% of hydroxypropyl cellulose (HPC), which adsorbs strongly on the glass surfaces, is also added to suppress electro-osmosis. The ac field is then applied parallel to these glass surfaces and the labeled molecules are observed by epifluorescence videomicroscopy perpendicularly to the slab cell. For strong ac fields (typically a few hundred V/cm at 100 Hz) the segregation gives rise to elongated ''aggregates'' (containing hundreds of λ-DNA fragments locally in semidilute regime) tilted with regard to the direction of the electric field. On a time scale of tens of seconds to a few minutes, these *tilted aggregates are actually quasistationary dynamical structures* within which individual DNA molecules recirculate continuously (see arrows on Fig. 3). The circulation velocity increases rapidly with the amplitude of the electric field and can reach 100 μm/s. The other main

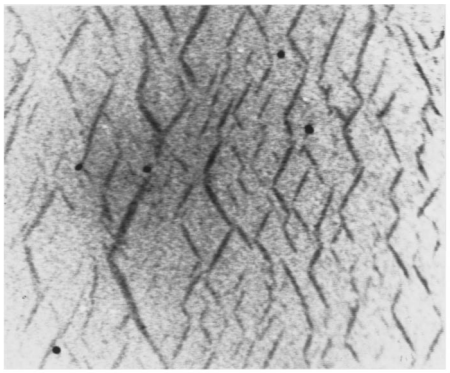

FIG. 2. Similar experiment as in Fig. 1 with a 300 V/cm ac field, in the horizontal direction, at the frequency 100 Hz. The angle of tilt between the direction of the electric field and the elongated aggregates is now $\theta\simeq\pm60°$ [2].

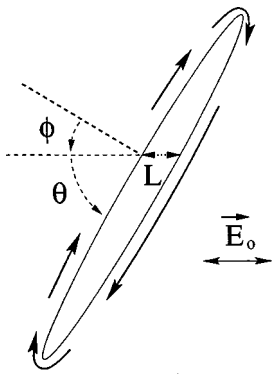

FIG. 3. Sketch of a field-induced quasistationary dynamical aggregate containing typically hundreds of macroions. The direction of circulation (arrows) changes with the sign of the tilt angle θ. The circulation velocity increases rapidly with increasing field, and can reach 100 μm/s close to the aggregate boundary.

features of these dynamical structures are the electric field ''threshold'' above which they are seen to develop within typically less than 1 min [1,2] and the precise value of their angle of tilt with respect to the direction of the electric field [4]. The field threshold decreases when the frequency is lowered or when the DNA molecular weight and, hence, the size of the coil are increased [1,2]. As for the tilt angle, one observes essentially two distinct values in the quasistationary dynamical regime developing over a few minutes after the onset of the instability [4]. At low frequency (i.e., $\omega/2\pi<10$ Hz), the periodic electrophoretic drift of the tilted aggregate is typically larger than its width, and we measure $\theta\simeq\pm45°$ (see Fig. 1 with $\omega/2\pi=2$ Hz). At higher frequency, the periodic drift of the tilted aggregate is smaller than its width, and we have $\theta\simeq\pm60°$ (see Fig. 2 with $\omega/2\pi=100$ Hz). Although tilted aggregates are often organized into zigzag patterns, this is not an essential feature of the instability since isolated tilted aggregates are also observed. Hopefully, these remarkable features should allow us to discriminate between different possible mechanisms for the physical origin of the phenomenon.

The description of electrophoresis of charged colloidal particles, i.e., their migration under electric field, has been a theoretical challenge for most of this century originating back in 1903 with the famous Smoluchowski expression giving the electrophoretic mobility, under weak electric field, of a charged sphere placed in a strong electrolyte of high ionic strength (i.e., $\kappa^{-1}\ll\ell$ where κ^{-1} is the Debye length and ℓ the sphere diameter) [8]. This states that the electric force on the particle essentially balances the viscous shear induced, within the Debye layer, by the excess counterions migrating under the electric field. Hence electrophoretic mobilities essentially reflect the basic electrokinetic phenomena at the Debye length scale.

Due to the complexity of the nonlinear electrokinetic equations, the electrophoretic mobility of a macroion is usually evaluated analytically assuming that the equilibrium distributions of the coions and counterions remain *unperturbed* under electric field *in the frame of reference of the migrating macroion*. Electrophoresis being, however, an out-of-equilibrium (dissipative) phenomenon, the equilibrium distributions of the electrolyte ions not only ''follow'' the migrating macroion but they are also perturbed in its vicinity under

the application of an electric field.

The perturbation of the ionic distributions *within* the Debye layers has been classically analyzed in linear theories taking the applied electric field as a small parameter as compared to the equilibrium electric field *within* the Debye layers [9]. It has been proposed [5,6] that the resulting polarization of the excess counterions in the Debye layers induces dipole-dipole *interactions* between the macroions, hence favoring macroscopic segregation of the dispersion for *thermodynamic* reasons [10]. We believe, however, that this mechanism alone is not sufficient to explain the *dynamical* features of the long recirculating tilted aggregates observed experimentally [4]. We do *not* invoke any further (dipole-dipole) interactions in this paper, concentrating instead on the *dynamical* processes originating from the perturbations of the ionic distributions *far beyond* the Debye layers, that is at length scales much larger than κ^{-1}, the Debye length of the electrolyte.

Classically, these small amplitude but large scale perturbations of the ionic distributions beyond the Debye layers are thought to be negligible in the limit of vanishing applied electric field (i.e., $E_0 \to 0$) since they appear to be of the order $O(E_0^2)$ as compared to the leading perturbations of the order $O(E_0)$ [9]. In fact this ''weak electric field'' result is contingent upon the *a priori* assumption that the equilibrium state (i.e., $E_0 = 0$) corresponds to the limit of the actual dynamical problem at vanishing applied electric field (i.e., $E_0 \to 0$). However, this limit may generally be singular, as we will show, and the validity of a straightforward expansion is questionable.

The plan of our discussion is the following: In Sec. II we discuss the electroneutrality breakdown beyond the Debye layer. We start by showing that the ionic concentrations are perturbed over large distances (i.e., wave vectors $k \ll \kappa$) in the vicinity of a single undeformable macroion under electrophoretic migration. In the dc regime, we find in particular that these perturbations correspond to a quasistationary salt depletion—in the vicinity of the moving macroion—which is globally *independent* of the amplitude of the applied electric field. We then argue that these out-of-equilibrium dynamical effects—better known in the context of electrodialysis with fixed charged membranes—lead to the breakdown of (equilibrium) electroneutrality beyond the Debye length scales.

In Sec. III we discuss large scale electrohydrodynamic flows in quasi-2D confined geometry. This large scale violation of strict electroneutrality eventually triggers, under electric field, some electrohydrodynamic flows within the colloidal dispersion that we first study in the large length scale ''Hele-Shaw'' approximation for a quasi-2D geometry. We propose in this section that the two angles of tilt of the elongated aggregates observed experimentally in this geometry (i.e., 45° and 60° at respectively low and high frequency) correspond in fact to two distinct dynamical limit regimes that can be described analytically.

In Sec. IV we discuss the electrohydrodynamic patterning process. The general problem of the three-charged-species system ''macroion, coion, and counterion'' is discussed with an emphasis on the separation of time scales between the fast dynamics of the small ions and the slow dynamics of the macroion density fluctuations. Although we find that this model does not exhibit ''classical'' instabilities (i.e., no exponential amplification of small perturbations around a perfectly uniform macroion distribution) we argue that the dynamics of the macroion density fluctuations is actually highly sensitive, at long time and large length scales, to the presence of thermal noise. This suggests that the observed electric-field-induced segregation might in fact correspond to a noise-driven instability as supported by some experimental evidence. We finally show, using numerical calculations, that the large scale electrohydrodynamic flows originating in the presence of preexisting inhomogeneous distributions of macroions are able to *dynamically* select some quasistationary patterns in good agreement with those observed experimentally. This is the strongest result supporting our approach.

II. ELECTRONEUTRALITY BREAKDOWN BEYOND THE DEBYE LAYER

Let us first consider a single *undeformable* macroion within a strong electrolyte solution. Being concerned here with the electrokinetic phenomena beyond the Debye layer we assume that the macroion charges can be described, at large length scales $k^{-1} \gg \kappa^{-1}$, by a smooth continuous concentration profile, $c_M(\vec{r},t)$. However, we also assume that the essential electrokinetic phenomena within the Debye layer of the actual macroion are satisfactorily taken into account by a phenomenological electrophoretic mobility, μ_M, relating the average electric field at the macroion scale, $\langle \vec{E} \rangle_M$, to its electrophoretic velocity $\vec{v}_e = z_M \mu_M \langle \vec{E} \rangle_M$ (conventionally we take unsigned electrophoretic mobilities with $z_M = \pm 1$ being the sign of the macroion' charges). In addition, we assume for simplicity that this primary electrophoretic motion is perfectly ''free-draining,'' that is, with no convective flow in the solution at larger scales than the Debye length, i.e., $\vec{v} = \vec{0}$ in the fixed frame of reference at length scales $k^{-1} \gg \kappa^{-1}$ [11].

Our aim is now to evaluate the first convective correction to this primary free-draining electrophoretic motion associated with the occurrence of electrohydrodynamic flows due to the large scale breakdown of local electroneutrality in the solution surrounding the macroion. We will argue in this section that this violation of electroneutrality at large length scales, i.e., $k^{-1} \gg \kappa^{-1}$, is related to the dynamical perturbation of the local salt concentration in the vicinity of the macroion under electrophoretic migration through the electrolyte solution.

A. Electrokinetic equations

The uniform transportation of the concentration profile, $c_M(\vec{r},t)$, describing the distribution of charges of the *undeformable* macroion can be written as

$$\partial_t c_M + (\vec{v}_e + \vec{v}_h) \cdot \vec{\nabla} c_M = 0, \tag{2.1}$$

where $\vec{v}_e = z_M \mu_M \langle \vec{E} \rangle_M$ is the macroion electrophoretic velocity defined above and $\vec{v}_h$ is the (weak) electrohydrodynamic convection of the solution, at the scale of the macroion, that we would eventually like to evaluate.

The uniform electrophoretic drift of the macroion then generates some out-of-equilibrium local perturbations of the

small coion and counterion concentrations since Poisson's equation (2.4) couples their conservation equations to the concentration profile of the macroion charges, $c_M(\vec{r},t)$. Namely,

$$\partial_t c_+ + \vec{\nabla}\cdot(-D_+\vec{\nabla}c_+ + \mu_+ c_+ \vec{E} + c_+\vec{v}) = 0, \quad (2.2)$$

$$\partial_t c_- + \vec{\nabla}\cdot(-D_-\vec{\nabla}c_- - \mu_- c_- \vec{E} + c_-\vec{v}) = 0, \quad (2.3)$$

$$\vec{\nabla}\cdot\vec{E} = \frac{e}{\varepsilon\varepsilon_0}(c_+ - c_- + z_M c_M) = \frac{\rho_e}{\varepsilon\varepsilon_0} \quad (2.4)$$

where $c_+(\vec{r},t)$, $c_-(\vec{r},t)$, D_+, D_-, and μ_+, μ_- are respectively the local concentrations, diffusion constants and absolute values of the electrophoretic mobilities of the small monovalent ions. e is the elementary charge, $\varepsilon\varepsilon_0$ the dielectric constant of the solution, and $\rho_e(\vec{r},t)$ is the local charge density. Finally, $\vec{v}$ is the *local* convection in the solution surrounding the macroion (which we distinguish in this section from $\vec{v}_h$, the convection *at the scale of the macroion*).

As this nonlinear system is also coupled—via $\vec{v}$—to some hydrodynamic equation—e.g., a Stokes-like equation—the general problem is a difficult task that can only be tackled within some approximation scheme.

B. Approximation scheme

As we already discussed in the Introduction, the classical perturbative approach to handle such an electrokinetic system is to make an expansion around the equilibrium state (no field applied) with respect to the amplitude of an applied electric field, supposedly small compared to the equilibrium electric field within the Debye layers [9]. However, since we are interested here in the electrohydrodynamic phenomena beyond the Debye layers—where the equilibrium electric field vanishes—we cannot resort to this classical ''low electric field'' approximation to overcome the complexity of the coupled nonlinear electrokinetic equations.

The alternative scheme we propose is to start from the far-from-equilibrium regime corresponding to the electrolyte solution *with no macroion* (i.e., $c_+ = c_- = c_s$) under some (strong) finite electric field $\vec{E}_0$. We then make an expansion around this uniform electrokinetic regime—writing $\vec{E} = \vec{E}_0 + \delta\vec{E}$, $c_+ = c_s + \delta c_+$, etc.—with respect to the supposedly small perturbations due to the macroion presence that we model, at large scales, by a smooth concentration profile of monovalent charges, $c_M(\vec{r},t)$—with $|\vec{\nabla}c_M|_{\max} \sim c_{M_{\max}}/\ell$, where ℓ is the macroion typical size, $\ell \gg \kappa^{-1}$. This approach requires in particular $c_{M_{\max}} \ll c_s$, which corresponds to a solution of high ionic strength. More precisely one can show (see below) that the ratio $c_{M_{\max}}/c_s$ can be taken as the small parameter to linearize the conservation equations (2.2) and (2.3) (i.e., $\delta E/E_0 \sim \delta c_+/c_s \sim \delta c_-/c_s \sim c_{M_{\max}}/c_s \ll 1$) when the applied electric field E_0 verifies the following condition:

$$\frac{eE_0\ell}{kT} \geqslant 1, \quad (2.5)$$

which ensures that the out-of-equilibrium perturbations dominate the equilibrium distributions $\delta\vec{E}^{\rm eq}$, $\delta c_-^{\rm eq}$ and $\delta c_+^{\rm eq}$, hence simplifying the discussion for the far-from-equilibrium regime. This condition typically holds for $E_0 \geqslant 100$ V/cm with $\ell \simeq 1$ μm and $c_{M_{\max}}/c_s \simeq 0.01$ corresponding to the experimental conditions reported for the observations on λ-DNA solutions [1,4,12].

Then linearizing and combining equations (2.2) and (2.3) to form the quantities $\mathcal{S} = \delta c_+ + \delta c_-$ and $\mathcal{R} = \delta c_- - \delta c_+$, and neglecting the convective term for $\mathcal{S}$ and $\mathcal{R}$ (i.e., assuming that $|\vec{v}| \ll D_s/\ell \simeq 1000$ μm/s) we obtain

$$\partial_t\mathcal{S} - D_s\Delta\mathcal{S} - \mu_s\vec{E}_0\cdot\vec{\nabla}\mathcal{R} = 0, \quad (2.6)$$

$$\partial_t\mathcal{R} - D_s\Delta\mathcal{R} - \mu_s\vec{E}_0\cdot\vec{\nabla}\mathcal{S} - \mu_s 2c_s\vec{\nabla}\cdot\delta\vec{E} = 0, \quad (2.7)$$

where we have assumed that $D_+ = D_- = D_s$ and $\mu_+ = \mu_- = \mu_s = D_s e/kT$ for simplicity [13].

As we are interested in evaluating the (large scale) deviations from electroneutrality, it is convenient to combine Eqs. (2.6) and (2.7) with Poisson's equation, $\rho_e = e(Z_M c_M - \mathcal{R}) = \varepsilon\varepsilon_0\vec{\nabla}\cdot\delta\vec{E}$, which gives

$$\partial_t\mathcal{S} - D_s\Delta\mathcal{S} = \mu_s\vec{E}_0\cdot\vec{\nabla}\left(z_M c_M - \frac{\rho_e}{e}\right), \quad (2.8)$$

$$z_M\partial_t c_M - z_M D_s\Delta c_M - \mu_s\vec{E}_0\cdot\vec{\nabla}\mathcal{S} = \frac{1}{e}(D_s\kappa^2\rho_e - D_s\Delta\rho_e + \partial_t\rho_e), \quad (2.9)$$

where we have introduced the expression for the Debye length in the electrolyte, $\kappa^{-1} = \sqrt{\varepsilon\varepsilon_0 kT/2e^2 c_s}$.

Although the coupled linear system can be exactly solved, we will gain more physical insight into the experimental situations of interest with some further approximations. At large length scales, $k^{-1} \gg \kappa^{-1}$, and long time scales, $t \gg 1/D_s\kappa^2$, we can evaluate the charge density ρ_e from Eq. (2.9) as

$$\rho_e = \frac{e}{D_s\kappa^2}(z_M\partial_t c_M - z_M D_s\Delta c_M - \mu_s\vec{E}_0\cdot\vec{\nabla}\mathcal{S}). \quad (2.10)$$

Using this result in Eq. (2.8) we then obtain, at these length and time scales (i.e., $k^{-1} \gg \kappa^{-1}$ and $t \gg 1/D_s\kappa^2$),

$$\partial_t\mathcal{S} - D_s\left[\Delta\mathcal{S} + \left(\frac{eE_0\kappa^{-1}}{kT}\right)^2\partial_y^2\mathcal{S}\right] = z_M\mu_s\vec{E}_0\cdot\vec{\nabla}c_M \quad (2.11)$$

where $\vec{E}_0$ is taken parallel to the y-axis.

In most practical situations we have $eE_0\kappa^{-1}/kT \ll 1$, which corresponds to a maximum electric field, $E_{0_{\max}} = kT/(e\kappa^{-1})$, generally much higher than any attainable experimental situation without turbulent heat convection or bubbles formation (e.g., $E_{0_{\max}} = 2\times10^5$ V/cm for $T \simeq 300$ K and $\kappa^{-1} \simeq 10^{-9}$ m). Hence, Eq. (2.11), describing the perturbation of the local salt concentration, can generally be further simplified to

$$\partial_t\mathcal{S} - D_s\Delta\mathcal{S} = z_M\mu_s\vec{E}_0\cdot\vec{\nabla}c_M. \quad (2.12)$$

These additional approximations actually amount to partially decoupling the linear system (2.8) and (2.9), which can now be solved in two successive steps: we first evaluate the local perturbation of the salt concentration with Eq. (2.12) [i.e., assuming electroneutrality in Eq. (2.8)] and the first correction to electroneutrality is then obtained, at large length and time scales, by substituting the result for $\mathcal{S}$ into Eq. (2.10).

C. Perturbation of the salt concentration

It is instructive to note that the perturbation in salt concentration due to the macroion presence is easily solved in the particular case of a 1D distribution of *fixed* charges, $c_M(y)$, perpendicularly to the direction of the electric field $\vec{E}_0$. If we also assume (for simplicity) a symmetric distribution around the origin, with a typical width L, we find a local quasi-stationary regime at long time scales $t \gg L^2/D_s$, in the region of the distribution (i.e., $|y| \leqslant L$),

$$\mathcal{S}(y,t) = -\frac{z_M e E_0}{kT} \int_0^y c_M(y')dy', \tag{2.13}$$

which corresponds to an antisymmetric profile with a net depletion of small ions on one side of the fixed distribution and an excess of salt on the other side. Then these concentration perturbations progressively extend by diffusion beyond the region of the fixed distribution, i.e., over the range $L \leqslant |y| \leqslant \sqrt{D_s t}$. This well known phenomenon, called electrodialysis, is in fact widely used to deionize electrolyte solutions by applying an electric current across (fixed) charged membranes.

We now turn to the case of a uniformly transported macroion, $c_M(\vec{r},t) \equiv c_M(\vec{r}-\vec{r}_0(t))$, where $\vec{r}_0(t)$ is the origin of the moving frame, i.e., $\dot{\vec{r}}_0(t) = \vec{v}_e + \vec{v}_h$ in Eq. (2.1). It is then convenient to take the Fourier transform of Eq. (2.12) defined as $\hat{\mathcal{S}}_{\vec{k}}(t) = \int\int\int \mathcal{S}(\vec{r},t) e^{i\vec{k}\cdot\vec{r}} d\vec{r}$, noticing that the Fourier components of the macroion profile, $\hat{C}_{\vec{k}}(t) = \int\int\int c_M(\vec{r}-\vec{r}_0(t)) e^{i\vec{k}\cdot\vec{r}} d\vec{r}$, can be written as

$$\hat{C}_{\vec{k}}(t) = e^{i\vec{k}\cdot\vec{r}_0(t)} \int\int\int c_M(\vec{r}\,') e^{i\vec{k}\cdot\vec{r}\,'} d\vec{r}\,' \equiv e^{i\vec{k}\cdot\vec{r}_0(t)} C_{\vec{k}}, \tag{2.14}$$

where $C_{\vec{k}}$ is independent of time for an undeformable migrating macroion. Hence, Eq. (2.12) becomes in Fourier space,

$$\partial_t \hat{\mathcal{S}}_{\vec{k}} + D_s k^2 \hat{\mathcal{S}}_{\vec{k}} = -z_M \mu_s \vec{E}_0 \cdot i\vec{k} C_{\vec{k}} e^{i\vec{k}\cdot\vec{r}_0(t)}. \tag{2.15}$$

We can similarly define the ''transported'' Fourier components of $\mathcal{S}$—in the reference frame of the moving macroion—as

$$\mathcal{S}_{\vec{k}}(t) = e^{-i\vec{k}\cdot\vec{r}_0(t)} \hat{\mathcal{S}}_{\vec{k}}(t), \tag{2.16}$$

which allows us to express Eq. (2.15) as

$$\partial_t \mathcal{S}_{\vec{k}} + i\vec{k}\cdot\vec{v}_0 \mathcal{S}_{\vec{k}} + D_s k^2 \mathcal{S}_{\vec{k}} = -Z_M \mu_s \vec{E}_0 \cdot i\vec{k} C_{\vec{k}}, \tag{2.17}$$

where $\vec{v}_0 = \dot{\vec{r}}_0(t)$ is the velocity of the migrating macroion. At linear order in $c_{M_{\max}}/c_s$, only the leading term of $\vec{v}_0$ should be kept in Eq. (2.17), that is, $\vec{v}_0 \simeq z_M \mu_M \vec{E}_0$.

For a dc field, the differential equation (2.17) is then tractable and gives, with the initial conditions $\mathcal{S}_{\vec{k}}(t=0) = \mathcal{S}^0_{\vec{k}}$,

$$\mathcal{S}_{\vec{k}}(t) = -\frac{z_M \mu_s \vec{E}_0 \cdot i\vec{k} C_{\vec{k}}}{D_s k^2 + z_M \mu_M \vec{E}_0 \cdot i\vec{k}} \left(1 - e^{-(D_s k^2 + z_M \mu_M \vec{E}_0 \cdot i\vec{k})t}\right) + \mathcal{S}^0_{\vec{k}} e^{-(D_s k^2 + z_M \mu_M \vec{E}_0 \cdot i\vec{k})t}. \tag{2.18}$$

At long time scales, $t \gg 1/D_s k^2$, the transported Fourier component $\mathcal{S}_{\vec{k}}(t)$ therefore becomes quasistationary,

$$\mathcal{S}_{\vec{k}} = -\frac{z_M \mu_s \vec{E}_0 \cdot i\vec{k}}{D_s k^2 + z_M \mu_M \vec{E}_0 \cdot i\vec{k}} C_{\vec{k}}. \tag{2.19}$$

For $t \gg \ell^2/D_s$, this implies that the electrophoretic migration of the macroion generates, in its vicinity, a quasistationary and asymmetric perturbation of the salt concentration. In particular, we note that $\mathcal{S}_{\vec{0}} = -(\mu_s/\mu_M)\int c_M d\vec{r} < 0$ corresponds to a global (out-of-equilibrium) depletion in salt *in the region of the macroion*. More precisely this requires taking the limit $t \to \infty$ first and then $k \to 0$ since $t \gg 1/D_s k^2$ is assumed in Eq. (2.19). In fact the total amount of salt is naturally conserved in the system [i.e., $\partial_t \mathcal{S}_{\vec{0}}(t) = 0$], however, the salt excess coming from the quasistationary depletion in the region of the moving macroion leads eventually to a vanishing increase in salt concentration in the rest of the solution since this is spread over a diverging volume at long time scales. One can get further physical insight into this salt depletion once realizing that it merely compensates for the (local) contribution of the moving macroion to the uniform total electric current as is immediately seen in the formal case, $\mu_s = \mu_M$ and $D_s = 0$ (then $\mathcal{S} = -c_M$). Finally, note that this quasistationary depletion in salt concentration in the vicinity of a macroion in electrophoretic migration, $\mathcal{S}_{\vec{0}}$, is *independent of the applied electric field*. Clearly, this type of singular dynamical behavior cannot be obtained within the classical theory of electrophoresis since the perturbations (from the equilibrium state) are then *constructed* to be proportional to the applied electric field E_0 [15].

D. Out-of-equilibrium deviations from electroneutrality

Once the salt profile has been determined, we then have the first correction to large scale electroneutrality from Eq. (2.10) and $\partial_t c_M \simeq -z_M \mu_M \vec{E}_0 \cdot \vec{\nabla} c_M$ [that is, Eq. (2.1) at first order in $c_{M_{\max}}/c_s$],

$$\rho_e = \varepsilon\varepsilon_0 \vec{\nabla}\cdot\delta\vec{E} \simeq \varepsilon\varepsilon_0 \left(-\frac{\mu_M}{\mu_s} \frac{\vec{E}_0 \cdot \vec{\nabla} c_M}{2c_s} - \frac{z_M kT}{e 2c_s} \Delta c_M - \frac{\vec{E}_0 \cdot \vec{\nabla}\mathcal{S}}{2c_s} \right). \tag{2.20}$$

The first term in the right-hand side of Eq. (2.20), depending explicitly on c_M, is the *dynamic* charge density arising in close vicinity to the *migrating* macroion (i.e., with $\mu_M \neq 0$) due to the time delay of the local electric relaxation where the macroion *passes through* the electrolyte [electric relaxation time: $1/D_s\kappa^2$ in Eq. (2.10)].

The second term of Eq. (2.20), depending also explicitly on c_M, is the approximate charge density at equilibrium (that is for $\vec{E}_0 = \vec{0}$) due to the macroion presence.

The strong electric field condition, $eE_0\ell/kT \geqslant 1$, ensures that the dynamic charges dominate the equilibrium charges at large scales, $k^{-1} \geqslant \ell$. In addition, Eq. (2.19) suggests that the first and the third terms in Eq. (2.20) have the same order of magnitude (as μ_M and μ_s have usually similar numerical values), which allows us to check, with Eq. (2.20), the consistency of the linearization conditions $\delta E/E_0 \sim \mathcal{S}/c_s \sim c_{M_{\max}}/c_s \ll 1$ announced earlier.

However, the net bulk charge corresponding to the third term, i.e.,

$$\rho_{e_{\mathcal{S}}} = -\varepsilon\varepsilon_0 \frac{\vec{E}_0 \cdot \vec{\nabla}\mathcal{S}}{2c_s} \tag{2.21}$$

typically extends over micrometers into the solution surrounding the moving macroion—that is, $k^{-1} \sim D_s/\mu_M E_0 \simeq 1-3\ \mu$m in Eq. (2.19). It is related to the variation of electric conductivity in the vicinity of the macroion due to the perturbation of the salt concentration, $\mathcal{S}$. One can visualize this large scale charge density $\rho_{e_{\mathcal{S}}}$ by stating that the small cation and anion concentration profiles, which add up to give the total salt profile, become shifted in opposite directions under $\vec{E}_0$ by a tiny distance δ' scaling as

$$\delta' = \frac{\varepsilon\varepsilon_0 E_0}{e2c_s} = \frac{eE_0\kappa^{-1}}{kT}\kappa^{-1}. \tag{2.22}$$

Although δ' is typically a picometric length, the associated polarization of the salt profile is enough to enforce a quasi-uniform electric current, $\vec{J} = (2c_s + \mathcal{S})(\vec{E}_0 + \delta\vec{E})$, in the solution surrounding the macroion as Eq. (2.20) becomes $\vec{\nabla}\cdot\vec{J} \simeq 0$ where $c_M = 0$. We will further argue in the following section that this apparently weak violation of local electroneutrality over micrometric scales, in the electrolyte solution surrounding the macroion, is also sufficient to lead to sustained electrohydrodynamic flows within the solution.

Finally we want to stress that the smooth macroion profile approximation we made is merely a handy toy model for which the applied electric field $\vec{E}_0$ dominates at all scales in the polyelectrolyte solution. A more physical model should explicitly take into account the usually much higher electric field within the Debye layer. We expect, however, that the electrokinetic phenomena beyond the Debye layer—where the electric field vanishes at equilibrium—should still correspond semiquantitatively to the physics we describe with this simple model.

III. LARGE SCALE ELECTROHYDRODYNAMIC FLOWS IN QUASI-2D CONFINED GEOMETRY

As already hinted at in the previous section, we expect that the breakdown of (equilibrium) electroneutrality in the solution surrounding the macroions generates, under strong electric field (to be estimated in the Sec. IV), electrohydrodynamic flows within the macroion dispersion. These flows are satisfactorily described by a Stokes-like equation at sufficiently low frequency of the electric field and in the regime for which the vorticity diffuses faster than the electrophoretic motion over the typical width, L, of the macroion aggregates [16]. This corresponds to $\nu/L^2 \gg \omega$ and $\nu/L^2 \gg \mu_M E_0/L$, where $\nu = \eta/\rho \simeq 10^{-6}$ m^2/s is the dynamical viscosity and ρ the mass density of the dispersion. For solutions of λ-DNA, we find that this regime corresponds to $\omega \ll \nu/L^2 \simeq 10^4$ Hz and $E_0 \ll \nu/(\mu_M L) \simeq 3\times 10^4$ V/cm, which clearly holds experimentally [1,4].

Hence, in this limit, we have the following relation between the (first order) local electric force $\rho_{e_{\mathcal{S}}}\vec{E}_0$ and the local velocity $\vec{v}$ in the electrolyte solution surrounding the macroions (see Appendix A):

$$\eta\Delta\vec{v} - \vec{\nabla}P + \rho_{e_{\mathcal{S}}}\vec{E}_0 = \vec{0}, \tag{3.1}$$

$$\text{with} \quad \rho_{e_{\mathcal{S}}} = -\varepsilon\varepsilon_0 \vec{E}_0 \cdot \vec{\nabla}\mathcal{S}/2c_s, \tag{3.2}$$

where η is the solvent viscosity and P the pressure in the solution. $\vec{v}$ also has to satisfy the incompressibility condition $\vec{\nabla}\cdot\vec{v} = 0$, and the boundary conditions $\vec{v} = \vec{0}$, at the macroion ''surfaces'' and at the recipient walls (that is in the laboratory frame if no electro-osmosis occurs). The flow $\vec{v}$ turns out to depend crucially on these boundary conditions for the dc regime that we have investigated until now, since the electric force behaves as a dipolelike term at large scales in this electrostatic analog equation [14], i.e., $|\rho_{e_{\mathcal{S}}}\vec{E}_0|(\vec{k}) \sim k$ as $k \to 0$ [from the Fourier transform of Eq. (2.21) and Eq. (2.19) at large scales $k^{-1} \gg D_s/\mu_M E_0$]. In particular we expect that experiments under different confined geometries will develop, in general, different dynamical structures.

In this section we limit our study to the quasi-2D confined geometry corresponding to the experimental conditions described in the Introduction. In such a geometry one usually makes the well-known Hele-Shaw approximation, which greatly simplifies the boundary condition problem on the two confining plates. It states that if $-\vec{\nabla}P + \rho_{e_{\mathcal{S}}}\vec{E}_0$ is essentially independent of z, the coordinate perpendicular to the confining plates, then the Stokes equation simplifies to the following 2D form at scales larger than $2a$, the separation distance between the plates:

$$-\frac{2\eta}{a^2}\vec{v}_{2\mathrm{D}}(x,y) - \vec{\nabla}_{2\mathrm{D}}P + (\rho_{e_{\mathcal{S}}}\vec{E}_0)_{2\mathrm{D}} = \vec{0}, \tag{3.3}$$

where $\vec{v}_{2\mathrm{D}}$ is in fact the maximum velocity of a Poiseuille profile between the plates: $\vec{v}(x,y,z) = (1 - z^2/a^2)\vec{v}_{2\mathrm{D}}(x,y)$.

Since the Hele-Shaw approximation holds for length scales larger than $2a$, we cannot consider individual macro-

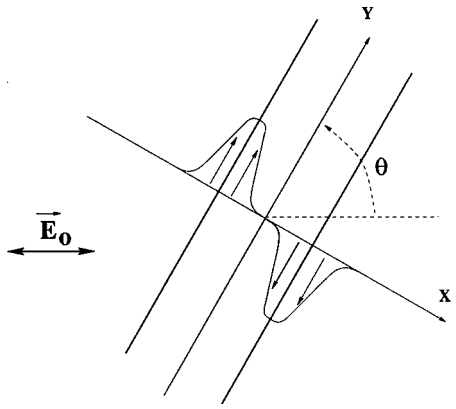

FIG. 4. Infinite band tilted with respect to the direction of the ac electric field $\vec{E}_0$. The electrohydrodynamic shearing at the (smooth) interfaces of the deformable band is drawn schematically.

ions anymore, assuming instead that macroion ''aggregates'' (or macroion density fluctuations), somewhat larger than $2a$, exist within the Hele-Shaw cell. At these scales, η is then the effective viscosity of the dispersion, which we assume to be independent of the macroion local concentration in a crude approach (i.e., leading order in $c_{M_{\max}}/c_s$). We postpone further discussion of the primary segregation process—from individual macroions to aggregates—to the next section.

For the sake of simplicity we will further assume in this section that the formed aggregates are quasi-infinite bands tilted with regard to the direction of the electric field in obvious reference to the experimental observations. Let us then assume that a quasi-infinite tilted bandlike aggregate of width L has formed in the Hele-Shaw cell. One can define a system of reference XY with the Y axis parallel to the band and we call θ the angle of tilt of the band with regards to the direction of the electric field ($|\theta|<90°$) (see Fig. 4).

We model this band as a whole by a smooth concentration profile of monovalent charges, $c_M(X,t)$, independent of Y and we use the fact that the primary electrokinetic phenomenon under electric field is still a uniform migration of the band with electrophoretic mobility μ_M, as for the case of a single macroion (see full discussion in the next section). Although the general electrokinetic problem is usually complex when an ac electric field is applied, we will now see that the situation is actually tractable in the two following limit regimes:

If the electric field frequency is smaller than the relaxation frequency of the salt perturbation, i.e., $\omega \leqslant D_s/L^2$, we expect that the theoretical approach developed for a macroion in the dc regime should also hold for the bandlike aggregate itself. In particular, for $\mu_M E_0 \sin(\theta)/L \geqslant D_s/L^2 \geqslant \omega$, the periodic drift of the band is larger than the bandwidth [i.e., $\mu_M E_0/\omega \geqslant L/\sin(\theta)$] and a quasi-dc salt depletion develops in the vicinity of the moving band. In practice this dc limit regime will apply for bandlike aggregates under low frequency ac field.

If the periodic drift of the band is smaller than its width [i.e., $\mu_M E_0/\omega \leqslant L/\sin(\theta)$] the associated perturbations of $c_M(X,t)$ are expected to be small. This will allow us to develop a perturbative approach for this ac limit regime corresponding to bandlike aggregates under high frequency ac electric fields.

Numerically, we find in fact, $D_s/L^2 \simeq \mu_M E_0/L \simeq 10$ Hz, which suggests that these regimes define, in practice, a simple partition of the frequency spectrum in apparent concordance with the low frequency ($\omega/2\pi < 10$ Hz) and high frequency ($\omega/2\pi > 10$ Hz) experimental regimes recalled in the Introduction [4]. We retain, however, in the following discussion, the less specific denomination of ''dc and ac limit regimes.'' Indeed we will argue in Sec. IV that these regimes also describe, at a given frequency, the physics at short length scales $k^{-1} < D_s k/\omega < \mu_M E_0/\omega$, and large length scales $k^{-1} > \max(\mu_M E_0/\omega, \sqrt{D_s/\omega})$, respectively.

A. The dc limit regime

Let us first consider the dc limit regime and apply the results, valid for a constant electric field, that we derived in Sec. II. We assume for simplicity that the aggregate is completely deformable at scales much larger than the size of the individual macroions, so that the convective electrohydrodynamics obeys Stokes equation (3.3) in the Hele-Shaw cell at large scales, i.e., $k^{-1} > a$. Taking the curl of Eq. (3.3) and introducing the stream function A ($\vec{v}_{2D} = \vec{\nabla} \times \vec{A}$ with $\vec{\nabla} \cdot \vec{A} = 0$ where $\vec{A} = A\hat{z}$), one finally gets in the transported Fourier space:

$$\vec{v}_{\vec{k}} = \frac{a^2}{2\eta} \frac{(-i\vec{k}) \times (-i\vec{k} \times \vec{E}_0)}{k^2} \rho_{e_{S\vec{k}}}. \tag{3.4}$$

Then using $\rho_{e_{S\vec{k}}} = (\varepsilon\varepsilon_0/2c_s)(i\vec{k} \cdot \vec{E}_0)\mathcal{S}_{\vec{k}}$, and $\mathcal{S}_{\vec{k}} \sim -(\mu_s/\mu_M)C_{\vec{k}}$ from Eq. (2.19) in the strong field limit $E_0 \gg D_s k/\mu_M$, we find,

$$\vec{v}_{\vec{k}} \sim \frac{\varepsilon\varepsilon_0}{2c_s} \frac{\mu_s}{\mu_M} \frac{a^2}{2\eta} (-i\vec{k} C_{\vec{k}}) \times \frac{(-i\vec{k} \times \vec{E}_0)(-i\vec{k} \cdot \vec{E}_0)}{k^2}. \tag{3.5}$$

This general result can easily be inverse Fourier transformed for the bandlike geometry. One obtains the following shearing flow at the band interfaces:

$$\vec{v}_{2D}(X) \sim \frac{\varepsilon\varepsilon_0}{2c_s} \frac{\mu_s}{\mu_M} \frac{a^2}{2\eta} E_0^2 \cos(\theta)\sin(\theta)[\hat{z} \times \vec{\nabla} c_M(X)]. \tag{3.6}$$

Note in particular that this flow is *parallel* to the band interface (Fig. 4) so that the associated convection of the deformable bandlike aggregate is indeed *stationary* [i.e., $\partial_t C_{\vec{k}}(t) = 0$] as was implicitly assumed in the derivation using the results of Sec. II for an undeformable macroion. The shearing velocity depends on the sign of the tilt angle θ in accordance with qualitative experimental observation, but is independent of z_M, the sign of the macroions' charges. Moreover the velocity amplitude predicted (up to a few tens μm/s) is in semiquantitative agreement with the experiments and, in practice, within the linearization condition $|\vec{v}| \ll D_s/L \simeq 100$ μm/s for $L \simeq a = 10$ μm.

In addition, we note that the stationary regime corresponding to the maximum shearing velocity occurs for the angle of tilt $\theta = \pm 45°$. We will discuss in the following sections this striking concordance with the observed tilt angle of

the aggregates in Fig. 1 (with $\omega/2\pi = 2$ Hz and $\sqrt{D_s/\omega} \simeq \mu_M E_0/\omega \simeq 3L$ corresponding indeed to the dc limit regime).

B. The ac limit regime

Consider now a tilted band of width L under an ac electric field, $\vec{E}_0(t) = \vec{E}_0 \cos(\omega t)$. The primary electrophoretic drift of the band is then (at leading order in $c_{M_{\max}}/c_s$),

$$\vec{r}_0(t) = z_M \mu_M \vec{E}_0 \frac{\sin(\omega t)}{\omega}. \tag{3.7}$$

In the ac limit regime, it is small compared to the bandwidth [i.e., $\mu_M E_0/\omega \ll L/\sin(\theta)$], and we have for large length scales $k^{-1} \gg |\vec{r}_0|$,

$$e^{i\vec{k}\cdot\vec{r}_0(t)} \simeq 1 + i\vec{k}\cdot\vec{E}_0 z_M \mu_M \frac{\sin(\omega t)}{\omega} + \cdots . \tag{3.8}$$

Using this approximation in Eq. (2.15) we obtain at long time scales, $t \gg L^2/D_s$, the following periodic perturbation of the salt profile in the region of the band:

$$\mathcal{S}_{\vec{k}}(t) \sim -i\vec{k}\cdot\vec{E}_0 z_M \mu_s C_{\vec{k}} \left[\frac{D_s k^2 \cos(\omega t) + \omega \sin(\omega t)}{D_s^2 k^4 + \omega^2} - i\vec{k}\cdot\vec{E}_0 \frac{z_M \mu_M}{2} \left(\frac{3 D_s k^2 \omega \sin(2\omega t)}{(D_s^2 k^4 + 4\omega^2)(D_s^2 k^4 + \omega^2)} + \frac{(D_s^2 k^4 - 2\omega^2)\cos(2\omega t)}{(D_s^2 k^4 + 4\omega^2)(D_s^2 k^4 + \omega^2)} + \frac{1}{(D_s^2 k^4 + \omega^2)} \right) + \cdots \right]. \tag{3.9}$$

This, in turn, generates a periodic bulk charge density under the ac field $\vec{E} = \vec{E}_0 \cos(\omega t)$ as [Eq. (2.21) in Fourier space]

$$\rho_{e_{\mathcal{S}\vec{k}}} \sim \frac{\varepsilon \varepsilon_0}{2 c_s} (i\vec{k}\cdot\vec{E}_0) \cos(\omega t) \mathcal{S}_{\vec{k}}(t) \tag{3.10}$$

and we finally get, after averaging $\mathcal{S}_{\vec{k}}(t)\cos^2(\omega t)$ over a period, an expression for the time averaged velocity. From Eq. (3.3), this gives at first order in μ_M [17] and for large length scales $k^{-1} \gg \sqrt{D_s/\omega}$ (one has also to make use of $\vec{\nabla} \times \delta\vec{E} = \vec{0}$ while taking the curl of Stokes equation)

$$\langle \vec{v}_{\vec{k}} \rangle \sim -\frac{3\varepsilon\varepsilon_0}{32 c_s} \frac{\mu_s \mu_M}{\omega^2} \frac{a^2}{2\eta} (-i\vec{k} C_{\vec{k}}) \times \frac{(-i\vec{k}\times\vec{E}_0)(-i\vec{k}\cdot\vec{E}_0)^3}{k^2}. \tag{3.11}$$

Hence,

$$\langle \vec{v}^{\,\mathrm{ac}}_{\vec{k}} \rangle \sim \vec{v}^{\,\mathrm{dc}}_{\vec{k}} \frac{3}{16} \left(\frac{\mu_M \vec{E}_0 \cdot \vec{k}}{\omega} \right)^2. \tag{3.12}$$

This decrease of the averaged convection velocity $\vec{v}$ with ω explains semiquantitatively why the observation of these electrohydrodynamic flows requires experimentally stronger electric fields if one increases the frequency [1].

Equation (3.11) can also be inverse Fourier transformed for the bandlike geometry. One obtains the following *stationary* shearing flow at the band interface:

$$\langle \vec{v}_{2\mathrm{D}} \rangle(X) \sim \frac{3\varepsilon\varepsilon_0}{32 c_s} \frac{\mu_s \mu_M}{\omega^2} \frac{a^2}{2\eta} E_0^4 \cos(\theta) \sin^3(\theta) \times (\hat{z}\times\hat{x}) \nabla^3 c_M(X). \tag{3.13}$$

As for the dc limit case, the shearing velocity is in semiquantitative agreement with the corresponding experiments: the direction of recirculation (depending on the sign of θ) is identical to that of the dc limit regime (see Fig. 4) and also independent of z_M, the sign of the macroions' charge. However, we note that the maximum shearing velocity of the band occurs now for a larger tilt angle, $\theta = \pm 60°$, for this ac limit case in concordance with the experiment of Fig. 2 (with $\omega/2\pi = 100$ Hz and $\mu_M E_0/\omega \simeq L/10$).

Interestingly, we note also that the electrohydrodynamics is much less sensitive to the boundary conditions in the ac limit regime, as compared to the dc limit regime, since the average electric momentum now behaves in Eq. (3.1) as an octopole at large scales, i.e., $|\rho_{e_{\mathcal{S}}}\vec{E}_0|(\vec{k}) \sim k^3$ as $k \to 0$. Hence we can study the case of an infinite polyelectrolyte solution in the ac limit regime.

Finally we emphasize again that the shearing regimes of the bandlike aggregates we have considered in this section are very specific dynamical regimes since the overall (bandlike) shape of the aggregate is globally preserved under the deformation. In contrast, we expect that, for a macroion aggregate of arbitrary shape, the electrohydrodynamic flow, originating from this macroion inhomogeneity, leads also to the deformation of the global shape of the macroion-rich domain itself [i.e., $\partial_t C_{\vec{k}}(t) \neq 0$]. This, in turn, will affect the geometry of the electrohydrodynamic flow, so that the global solution will eventually undergo some complex evolution. The study of these dynamical processes is attempted in the following section.

IV. ELECTROHYDRODYNAMIC PATTERNS

The aim of this last section is to present a unified approach investigating these electrohydrodynamic ''instabilities'' for the three-charged-species model: macroions, coions, and counterions. In the next subsection, we introduce

an additional equation to the general electrohydrokinetic system discussed in Secs. II and III, to describe the dynamics of the macroion density fluctuations within the electrolyte solution. We argue that this kinetic equation contains—in some limit—the essential nonlinearities of the system that can be solved, at long time scales, with the quasistatic responses of the small ion distributions and the electrohydrodynamic Stokes flow. We find that this three-charged-species model is linearly stable when the effects of stochastic fluctuations are neglected. However, we then argue that the nonlinear electrohydroconvective term $(\vec{v}\cdot\vec{\nabla}c_M)$ actually dominates the long time, large scale dynamics of the macroion distribution when these stochastic effects are included in the description of the macroion dynamics. This suggests that the electric-field-induced segregation might in fact be a noise-driven dynamical process as supported by some experimental evidence (Sec. IV A). We leave aside, however, further quantitative discussion of this delicate noise-driven mechanism far away from the equilibrium homogeneous state of the dispersion. Finally, we demonstrate numerically the ability of our model to account for the formation of quasistationary dynamical structures from a preexisting inhomogeneous macroion distribution in a Hele-Shaw cell. These numerical results are in good agreement with corresponding experimental observations (Sec. IV B).

A. A three-charged-species model

1. Electrokinetic equations

Let us call ν_M, the local *macroion concentration* in the electrolyte. We first follow the usual approach assuming that the dynamics of the local concentrations can be described neglecting the effects of stochastic fluctuations. We therefore expect ν_M to verify at large scales, $k^{-1}\gg 1/\langle\nu_M\rangle^{1/3}$, the following dynamic equation (called the Smoluchowski equation):

$$\partial_t\nu_M+\vec{\nabla}\cdot(-D_M\vec{\nabla}\nu_M+z_M\mu_M\nu_M\vec{E}+\nu_M\vec{v})=0, \quad (4.1)$$

where D_M and $z_M\mu_M$ are respectively the diffusion constant and the electrophoretic mobility of the macroions. At these scales we also have $\nu_M=c_M/N_M$, where c_M is the concentration profile of the (monovalent) charges associated with the macroions and, N_M the number of elementary charges per macroion. Hence the complete three-charged-species electrohydrodynamic system can be modeled with three conservation equations,

$$\partial_t c_+ +\vec{\nabla}\cdot(-D_+\vec{\nabla}c_+ +\mu_+ c_+\vec{E}+c_+\vec{v})=0, \quad (4.2)$$

$$\partial_t c_- +\vec{\nabla}\cdot(-D_-\vec{\nabla}c_- -\mu_- c_-\vec{E}+c_-\vec{v})=0, \quad (4.3)$$

$$\partial_t\nu_M+\vec{\nabla}\cdot(-D_M\vec{\nabla}\nu_M+z_M\mu_M\nu_M\vec{E}+\nu_M\vec{v})=0, \quad (4.4)$$

where the nonlinear electrophoretic currents couple these dynamic relations to Maxwell's electrostatic relations (in the absence of magnetic field),

$$\vec{\nabla}\cdot\vec{E}=\frac{e}{\varepsilon\varepsilon_0}(c_+-c_-+z_Mc_M)=\frac{\rho_e}{\varepsilon\varepsilon_0}, \quad (4.5)$$

$$\vec{\nabla}\times\vec{E}=\vec{0}, \quad (4.6)$$

whereas the nonlinear convection currents require some further electrohydrodynamic constitutive relation coupling the local flow $\vec{v}$ to the ionic concentrations and the local electric field in the solution (note that $\vec{v}_h\equiv\vec{v}$ at these length scales $k^{-1}\gg 1/\langle\nu_M\rangle^{1/3}$; see Sec. II). As a crude model we assume that this can be accounted for, at large scales, by a simple Stokes-like equation,

$$\eta\Delta\vec{v}-\vec{\nabla}P+\rho_{e_S}\vec{E}=\vec{0}, \quad (4.7)$$

where η is an effective viscosity and ρ_{e_S} the charge density in the electrolyte solution surrounding the macroions as discussed in Sec. II (see also Appendix A and [16]). This flow must also verify the incompressibility condition $\vec{\nabla}\cdot\vec{v}=0$, and the appropriate boundary conditions at the rigid walls. The resulting nonlinear partial differential equations (PDE) system [Eqs. (4.2), (4.3), (4.4), (4.5), (4.6), and (4.8)] is clearly not tractable analytically in the general case and approximations are necessary to allow further progress.

2. Approximation scheme

Let us first consider the large scale electrohydrodynamics within a Hele-Shaw cell of thickness $2a$ $(k^{-1}\gg a)$, which we introduced above. In this quasi-2D confined geometry we get, introducing the vector potential $\vec{A}=A(x,y)\hat{z}$ perpendicular to the confining plates [with $\vec{v}_{2D}(x,y)=\vec{\nabla}\times\vec{A}$],

$$-\frac{2\eta}{a^2}\Delta\vec{A}+\vec{\nabla}\rho_{e_S}\times\vec{E}_0=\vec{0}, \quad (4.8)$$

where we have used Maxwell's equation (4.6) and $\vec{\nabla}\cdot\vec{A}=0$.

Although the simplified nonlinear general system [Eqs. (4.2), (4.3), (4.4), (4.5), and (4.8)] is still not tractable analytically we can further progress as we are interested here in particular situations with (large) macroions diffusing much more slowly than the (small) coions and counterions. Typically, this corresponds to $D_M\simeq D_s/1000\simeq 10^{-12}$ m^2/s for macroions in the micrometer range, whereas the electrophoretic mobilities (μ_-, μ_+, and μ_M) have usually similar numerical values at high ionic strength. Hence the relative weight of the stabilizing diffusive term is much less important in the macroion dynamical equation than in the corresponding equations for the small ions. This means that the nonlinearities of the electrophoretic and convective currents are potentially much more destabilizing for the macroions [Eq. (4.4)] than for the small ions [Eqs. (4.2) and (4.3)]. We therefore expect that, at some intermediate electric field, the essential nonlinearities of the system lie in the macroion Smoluchowski equation (4.4) whereas the conservation equations for the small ions can be linearized as discussed in Sec. II [Eqs. (2.6) and (2.7)]. Namely,

$$\partial_t\mathcal{S}-D_s\Delta\mathcal{S}-\mu_s\vec{E}_0\cdot\vec{\nabla}\mathcal{R}=0, \quad (4.9)$$

$$\partial_t\mathcal{R}-D_s\Delta\mathcal{R}-\mu_s\vec{E}_0\cdot\vec{\nabla}\mathcal{S}-\mu_s 2c_s\vec{\nabla}\cdot\vec{\delta E}=0, \quad (4.10)$$

$$\partial_t \nu_M + z_M \mu_M \vec{E}_0 \cdot \vec{\nabla} \nu_M + \vec{\nabla} \cdot (-D_M \vec{\nabla} \nu_M + z_M \mu_M \nu_M \delta\vec{E} + \nu_M \vec{v}) = 0, \quad (4.11)$$

where we again assumed, $D_+ = D_- = D_s$ (with $D_s \gg D_M$) and $\mu_+ = \mu_- = \mu_s = D_s e/kT$ for simplicity [13]. As previously we define $\mathcal{S} = \delta c_+ + \delta c_-$ and $\mathcal{R} = \delta c_- - \delta c_+$.

Hence the nonlinear dynamic equation for the macroions [Eq. (4.11)] is now coupled (via $\delta\vec{E}$ and $\vec{v}$) to a *linear* PDE system [Eqs. (4.5), (4.8), (4.9), and (4.10)]. Although the global system remains insoluble analytically, we can still progress with further approximations as we will now discuss. Consider some large scale spontaneous fluctuation of the macroion distribution with typical wave vector k ($k^{-1} \gg a$). Under strong electric field we expect—from the discussion of Sec. II—that the primary electrophoretic motion of this macroion density fluctuation generates some large scale perturbations of the salt concentration. If we further assume that the dynamical evolution of this macroion density fluctuation is much slower (in the electrophoretic moving frame) than the response of the salt distribution (i.e., if significant evolutions of the macroion distribution occur at long time scales $t \gg 1/D_s k^2$) we can then estimate the electric field perturbation $\delta\vec{E}$ and the electrohydrodynamic convection $\vec{v}$ using the results of Secs. II and III where we assumed a uniform electrophoretic transportation of some undeformable macroion profile: $c_M(\vec{r},t) \equiv c_M(\vec{r} - \vec{r}_0(t))$.

Using Eq. (2.20) and, e.g., Eq. (3.6) to estimate $\delta\vec{E}$ and $\vec{v}$, respectively, one can then check that this assumption of ''quasistatic'' salt perturbation (in the moving frame) is usually well verified in practical situations (that is, $D_M k$, v, $\mu_M \delta E \ll D_s k$). Hence, the long time dynamics of the macroion distribution can be estimated, in the moving frame ($d_t \equiv \partial_t + z_M \mu_M \vec{E}_0 \cdot \vec{\nabla}$), by the following nonlinear dynamic equation:

$$d_t \nu_M - D_M \Delta \nu_M + z_M \mu_M \vec{\nabla} \cdot (\nu_M \delta\vec{E}) + \vec{v} \cdot \vec{\nabla} \nu_M = 0, \quad (4.12)$$

where $\delta\vec{E}(\nu_M)$ and $\vec{v}(\nu_M)$ are evaluated, as in Secs. II and III, by solving the remaining linear PDE system [Eqs. (4.5), (4.8), (4.9), and (4.10)] with the assumption that, under a strong electric field $\vec{E}_0$, the short time scale dynamics of ν_M is a uniform electrophoretic migration, i.e., $d_t \nu_M = \partial_t \nu_M + z_M \mu_M \vec{E}_0 \cdot \vec{\nabla} \nu_M \simeq 0$, as for the case of an undeformable macroion (Sec. II).

From Secs. II and III we have the following in Fourier space (with $\nu_{\vec{k}} = C_{\vec{k}}/N_M$).

(i) In the dc limit case, i.e., $k^{-1} \ll D_s k/\omega < \mu_M E_0/\omega$,

$$\vec{v}^{\,\mathrm{dc}}_{\vec{k}} \sim N_M \frac{\varepsilon\varepsilon_0}{2c_s} \frac{\mu_s}{\mu_M} \frac{a^2}{2\eta} (-i\vec{k}\nu_{\vec{k}}) \times \frac{(-i\vec{k} \times \vec{E}_0)(-i\vec{k} \cdot \vec{E}_0)}{k^2}, \quad (4.13)$$

$$\delta\vec{E}^{\,\mathrm{dc}}_{\vec{k}} \sim -N_M \left(\frac{\mu_s}{\mu_M} - \frac{\mu_M}{\mu_s} \right) \frac{-i\vec{k} \cdot \vec{E}_0}{k^2} \frac{-i\vec{k}\nu_{\vec{k}}}{2c_s}. \quad (4.14)$$

(ii) In the ac limit case, i.e., $k^{-1} \gg \max(\mu_M E_0/\omega, \sqrt{D_s/\omega})$,

$$\langle \vec{v}^{\,\mathrm{ac}}_{\vec{k}} \rangle \sim -N_M \frac{3\varepsilon\varepsilon_0}{32c_s} \frac{\mu_s \mu_M}{\omega^2} \frac{a^2}{2\eta} (-i\vec{k}\nu_{\vec{k}}) \times \frac{(-i\vec{k} \times \vec{E}_0)(-i\vec{k} \cdot \vec{E}_0)^3}{k^2}, \quad (4.15)$$

$$\langle \delta\vec{E}^{\,\mathrm{ac}}_{\vec{k}} \rangle \sim N_M \frac{z_M kT}{e 2c_s} i\vec{k}\nu_{\vec{k}}. \quad (4.16)$$

3. Linear stability

Let us first consider some small spontaneous fluctuation, $\delta\nu_M$, around the uniform macroion concentration, ν_M^0. From Eq. (4.12) we find that $\delta\nu_M$ follows at first order the following dynamical equation [since $\delta\vec{E}(\nu_M^0) = \vec{0}$ and $\vec{v}(\nu_M^0) = \vec{0}$]:

$$d_t \delta\nu_M - D_M \Delta \delta\nu_M + z_M \mu_M \nu_M^0 \vec{\nabla} \cdot \delta\vec{E} = 0, \quad (4.17)$$

which becomes in the dc limit regime [using Eq. (4.14)]

$$\left[d_t + z_M \left(\mu_s - \frac{\mu_M^2}{\mu_s} \right) \frac{N_M \nu_M^0}{2c_s} \vec{E}_0 \cdot \vec{\nabla} \right] \delta\nu_M - D_M \Delta \delta\nu_M = 0 \quad (4.18)$$

and in the ac limit regime [using Eq. (4.16)],

$$d_t \delta\nu_M - \left(D_M + \frac{N_M \nu_M^0}{2c_s} \frac{\mu_M kT}{e} \right) \Delta \delta\nu_M = 0. \quad (4.19)$$

This shows that ν_M does not exhibit any ''classical'' instability in the small ions' ''quasi-static'' response approximation since no exponential amplification of small modulations—around the perfectly uniform distribution ν_M^0—is predicted from Eqs. (4.18) and (4.19). In fact, one can show by a straightforward but tedious calculation [18] that the general system, Eqs. (4.2), (4.3), (4.4), and (4.5), is itself linearly stable. We will, however, argue in the following subsection that the actual three-charged-species system might nonetheless be ''unstable'' once we take into account the so far neglected effects of stochastic fluctuations on the macroion dynamics.

4. Noise-driven pattern formation

The formation of interesting noise-driven patterns has already been shown to arise from nonlinear stochastic PDE with no deterministic destabilizing term. The idea originated with the seminal paper of Kardar, Parisi, and Zhang [19] who proposed that interfaces growing under noisy ballistic deposition of particles undergo some *kinetic roughening* following *universal dynamic scaling laws* due to the large scale dominance of a nonlinear term in the stochastic equation describing the deposition process (see also [20]).

In the general case, the ''stability'' of the large scale behavior of the linearized stochastic equation against the inclusion of nonlinear terms can be probed by the simple technique referred to as *power counting* introduced in the context of the renormalization group theory. Nonlinear terms whose importance at long time and large scales vanishes under rescaling are said to be *irrelevant* for the long time, large length scale dynamics of the system and can usually be omitted. On

the other hand, nonlinear terms ''growing'' under dynamic rescaling cannot be generally neglected (in contradiction with the classical analysis of linear stability) since they modify the long time, large scale dynamical behavior of the system.

A more quantitative analysis involving dynamical renormalization calculations [19,21] relies, however, on the assumption that the stochastic properties of the (leading) noise term are invariant under rescaling. This condition can conceivably be fulfilled when the noise source is *external* to the otherwise deterministic system as in the case of a growing interface under random deposition of particles [19]. This is to be contrasted with the case of systems exhibiting *internal* noise [22] that typically originates from the fact that they consist of discrete thermally agitated particles, as for the three-charged-species system in which we are interested in this paper. Indeed the effect of such internal noise on nonlinear systems leads to delicate conceptual questions [23] and we expect in particular that internal noise sources change their stochastic properties under dynamical rescaling. Still, at a qualitative level, we can identify the potential relevance of the inclusion of nonlinear terms against the presence of an (internal) noise source with specific stochastic properties.

The primary internal noise we are interested in to test the relevance of the nonlinear terms in our three-charged-species system is clearly the thermal noise responsible for the thermodynamic fluctuations at equilibrium. For simplicity, we will limit our discussion to the (realistic) asymptotic regime where the effects of stochastic fluctuations and nonlinear terms are restricted to the dynamic equation of the slow diffusing macroions (with ''quasistatic'' responses of the small ions, as previously discussed). Following van Vliet's approach to density fluctuations in diffusive systems [24] we therefore add to the deterministic linearized equations (4.18) and (4.19) the (thermal) noise source $f(\vec{r},t)$ with the following first two moments:

$$\langle f(\vec{r},t)\rangle = 0, \tag{4.20}$$

$$\langle f(\vec{r},t) f(\vec{r},t')\rangle \sim -2D_M \nu_M^0 \nabla^2 \delta^d(\vec{r}-\vec{r}')\,\delta(t-t'), \tag{4.21}$$

or in Fourier space

$$\langle f(\vec{k},t) f(\vec{k}',t')\rangle \sim 2D_M \nu_M^0 k^2 \delta^d(\vec{k}+\vec{k}')\,\delta(t-t'), \tag{4.22}$$

where d is the spatial dimension. This leads in particular to the expected thermodynamic density fluctuations for an ''ideal gas'' of macroions (since all interactions have been neglected),

$$\frac{\langle \delta\nu_M^2\rangle^{1/2}}{\nu_M^0} \sim \frac{1}{\sqrt{\nu_M^0 V}}, \tag{4.23}$$

where V is the volume of the observed subsystem.

The study of the relevance of the nonlinear terms $\vec{\nabla}\cdot(\delta\nu_M \delta\vec{E})$ and $\vec{v}\cdot\vec{\nabla}\delta\nu_M$ added to the linearized stochastic equation for the macroion density fluctuations is performed in Appendix B. As we have mentioned in Sec. III, the ''aggregation'' between individual macroions should already occur at smaller length scales than the distance a between the confining surfaces of the Hele-Shaw cell. Below this hydrodynamic screening length, we estimate the behavior of the electrohydrodynamic flow by changing $2/a^2$ into k^2 in the Stokes equation (that is, assuming a perfectly infinite system without hydrodynamic boundary conditions).

For the spatial dimension of interest here, $d=3$, we find (see Appendix B) that the non-linear term $\vec{\nabla}\cdot(\delta\nu_M\delta\vec{E})$ is always *irrelevant* whereas the electrohydroconvective term $\vec{v}\cdot\vec{\nabla}\delta\nu_M$ is *relevant* in the *unscreened* dc limit regime (i.e., $k^{-1}<a$ and $k^{-1}\ll D_s k/\omega < \mu_M E_0/\omega$) but *irrelevant* in all the other regimes (i.e., screened dc limit, screened and unscreened ac limit regimes). This result demonstrates that the diffusive stabilizing term $-D_M\Delta\delta\nu_M$ is not sufficient to ensure the stability of an initially homogeneous macroion distribution in the presence of both stochastic fluctuations and electrohydroconvection [25]. This suggests that the nonlinear convective term may actually have a crucial role in the dynamical processes within the macroion dispersion (as supported by simple estimations of orders of magnitude in the situations corresponding to the experimental conditions; see Appendix C). In general, we therefore expect that this electroconvective term might generate some large scales dynamic patterns from the spontaneous thermal fluctuations in the macroion dispersion.

On the qualitative level this dynamical segregation process would be able to account for the following important experimental observations [27]:

(1) Under dc or low frequency ac electric field conditions the solution undergoes some *coarse graining* process generating denser macroion regions until the size of the globular segregated regions typically reaches the spacing length a between the confining walls, that is, the hydrodynamic screening length. The fast coarse graining process then stops in apparent agreement with the *irrelevance* of the nonlinear convective term at larger scales $k^{-1}\geqslant a$, as we cross from a 3D unscreened hydrodynamic regime to a screened one (in a Hele-Shaw cell or capillaries [1]).

(2) At higher frequency, when the periodic drift of the macroions is smaller than the typical hydrodynamic screening length a enforced by the experiment geometry, we observed that the coarse graining process may stop in the direction of the electric field before it reaches the size a, as is clearly visible in the observations on DNA solutions in capillaries showing disk-shape aggregates thinner than the capillary diameter a [1]. In the dynamic scaling picture this would correspond to the crossover of the nonlinear convective term from its *relevant* (dc limit) behavior at short length scales (i.e., for $k^{-1}<D_s k/\omega<\mu_M E_0/\omega<a$) to its *irrelevant* (ac limit) behavior at larger scales (i.e., for $k^{-1}>\mu_M E_0/\omega$).

(3) Finally the comparison between this *relevant* nonlinear term $\vec{v}\cdot\vec{\nabla}\nu_M$ in the unscreened dc limit and the diffusive stabilizing term $-D_M\nabla^2\nu_M$ is expected to give some order of magnitude of the experimental electric field threshold for this electric-field-induced ''segregation'' to occur. Taking $k^{-1}\simeq\langle\nu_M\rangle^{-1/3}$ and $D_M\simeq kT/(\eta R_g)$, we find

$$E_T \simeq \sqrt{\frac{kTc_s}{\varepsilon\varepsilon_0 R_g N_M \langle\nu_M\rangle^{1/3}}} \tag{4.24}$$

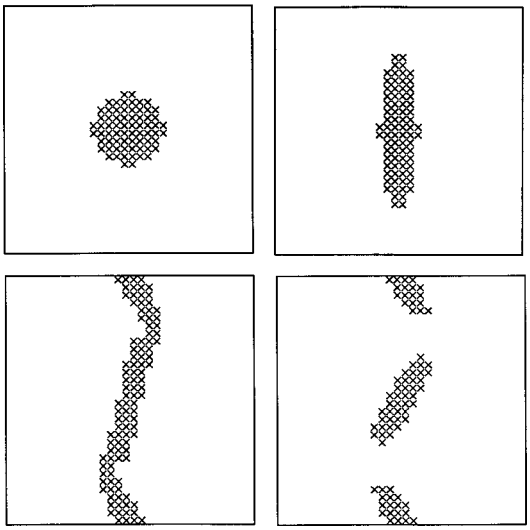

FIG. 5. Numerical evolution of an initially Gaussian macroion distribution induced by the application of a strong (horizontal) electric field in the analytic ac limit regime. Spatial periodic boundary conditions are used. Time scales (when the known values of the experimental parameters are used): (A) $t=0$ s; (B) $t=0.1$ s; (C) $t=1.5$ s; (D) $t=3$ s (quasistationary regime). ''×'' indicates that the local probability density is at least one-tenth of the maximum of the initial distribution.

for a dilute solution of macroions. Numerically, E_T is a few tens of V/cm for a 30 μg/ml λ-DNA solution in good agreement with the experimental onset of aggregation. Note also that E_T decreases with the macroion size (R_g), charge (N_M), and concentration (ν_M) in qualitative agreement with the experimental observations [1].

More quantitative progress requires, however, the use of more sophisticated techniques such as the dynamic renormalization group theory and we do not address further the aggregation problem here [28].

B. Numerics

Although we have seen in the last subsection that Eq. (4.12) does not account for the primary segregation process, we still expect it to give us some understanding of the large scale evolution of a preexisting macroion-rich segregated region under strong electric field. We have therefore solved Eq. (4.12) numerically, in the Hele-Shaw approximation, for some initially segregated domains of simple shape. The calculations are performed in Fourier space with an extensive use of the fast Fourier transform algorithm [29].

Figure 5 shows the time evolution in the ac limit regime of an initially 2D Gaussian distribution of macroions [i.e., Eqs. (4.15) and (4.16) have been used to evaluate $\vec{v}_{\vec{k}}(\nu_M)$ and $\delta\vec{E}_{\vec{k}}(\nu_M)$ respectively]. The known experimental values of the various physical parameters have been used in the calculation and the electric field frequency and amplitude have been chosen to correspond typically to the experimental ac limit regime, namely, $E_0=500$ V/cm and $\omega/2\pi=100$ Hz. Within a tenth of second the initial Gaussian distribution is symmetrically elongated perpendicularly to the direction of the (horizontal) electric field. This is due to the convective electrohydrodynamic flow, which is shown to dominate the macroion fluctuation dynamics in this regime (see Appendix C). After about 1 s, the symmetry of the deformation is spontaneously broken and a quasistationary dynamical regime is reached, exhibiting elongated aggregates tilted with respect to the direction of the electric field. Finally, after a few more seconds, the diffusion slowly wins over the long time scale dynamics as expected in the Hele-Shaw approximation (see previous section) and the tilted aggregates progressively disappear. Remarkably, we note that the quasistationary regime corresponds to a $\pm 60°$ tilt angle of the elongated dynamical aggregates with respect to the field, which we identified in Sec. III as the stationary regime corresponding to the *maximum shearing of the bandlike aggregates*. This suggests that these quasistationary dynamical structures are actually generated and sustained by an *abrasion* mechanism at the aggregate interface that tends to ''facet'' the macroion-rich regions at the angle corresponding to the most efficient abrasion process, that is, $\theta=\pm 60°$ in the ac limit regime. Such a mechanism is indeed expected to dynamically whittle down or gradually cover the interfacial regions of the aggregate that are not oriented along the direction of fastest electrohydrodynamic convection at the interface, thus eventually faceting the whole aggregate along these directions of most efficient abrasion process.

The system dimensions, combined with the periodic boundary conditions we have used in the numerical calculations, tend to fix the zigzag pattern periodicity for systems of medium sizes, as shown in Fig. 5, however, we checked—performing (less accurate) calculations in bigger systems—that these chevron-like patterns can appear even before the deformation of the macroion-rich region reaches the system ''edges'' (data not shown).

This numerical solution of the large scale evolution of an initially Gaussian macroion-rich region is clearly in good agreement with the corresponding experiment depicted on Fig. 6. In this experiment, a DNA aggregate, previously formed under strong electric field, has been left to diffuse for about 1 minute after the electric field was turned off. A strong electric field is then reapplied on the disk-like macroion-rich region ($E_0=500$ V/cm and $\omega/2\pi=100$ Hz), which deforms first perpendicularly to the (horizontal) electric field. However, this symmetric elongation is unable to lead to any stationary dynamical regime and the aggregate eventually breaks, after about 1 s (by spontaneous fluctuation), to form a stable quasistationary zigzag pattern where the continuously sheared long aggregates have indeed a $\pm 60°$ angle of tilt with respect to the field as for the case of Fig. 2 corresponding also to the ac limit regime (but starting initially from a dispersion at equilibrium, i.e., with thermodynamic fluctuations).

Figure (7) is the numerical quasistationary dynamical structure formed, in the dc limit regime, from an initially Gaussian macroion distribution. The $\pm 45°$ angle of tilt between the continuously sheared long aggregates and the electric field also clearly demonstrates good agreement with Fig. 1, depicting the experimental observations in the dc limit conditions.

V. CONCLUSION

We have developed in this paper the basis of a theoretical approach to describe the *large scale, long time* electrohydro-

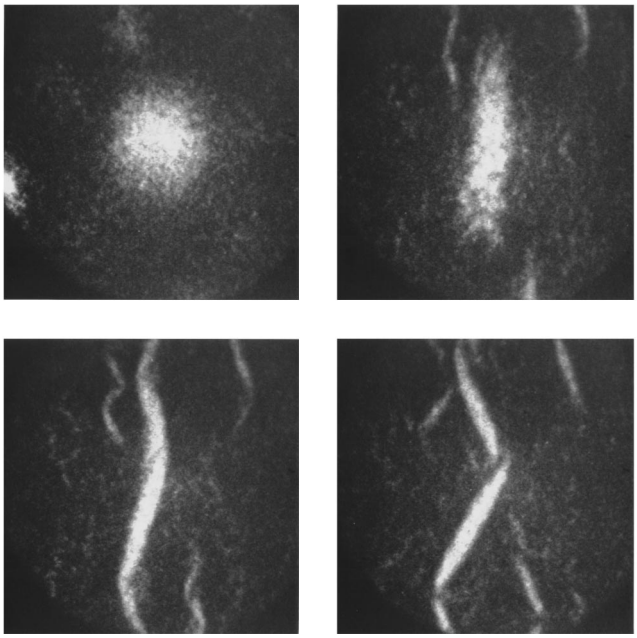

FIG. 6. Experimental evolution of an initially quasi-isotope λ-DNA-rich region (about 10 μm in diameter) under the sudden application of a strong ac electric field in the horizontal direction: field amplitude 500 V/cm and frequency 100 Hz. (A) $t=0$ s; (B) $t=0.5$ s; (C) $t=1.5$ s; (D) $t\geqslant 3$ s (quasistationary regime).

kinetic phenomena occurring, under strong electric field, in a dispersion of macroions in a simple electrolyte of high ionic strength.

The main ideas and approximations of this approach can be summarized as follows.

(i) The macroions' charges are described, at large length scales, by a smooth concentration profile, $c_M(\vec{r},t)$, depending *a priori* on the space and time coordinates, and the short scale electrokinetic phenomena are taken into account phenomenologically by the introduction of an electrophoretic mobility μ_M for the macroions.

(ii) The difficulties of the coupled nonlinear electrokinetic equations are overcome by considering that the macroions merely generate small perturbations on the already out-of-equilibrium situation of the simple electrolyte ($c_+=c_-=c_s$) under a strong electric field, $\vec{E}_0$. We then use the supposedly small parameter c_M/c_s (electrolyte of high ionic strength) to expand the nonlinearities in the coupled equations.

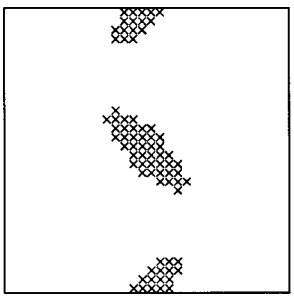

FIG. 7. Numerical quasistationary structure, obtained from the evolution of an initially Gaussian macroion distribution (as in Fig. 5), induced by the application of a strong (horizontal) electric field in the analytic dc limit regime. Spatial periodic boundary conditions are used. ''×'' indicates that the local probability density is at least one-tenth of the maximum of the initial distribution.

(iii) As the macroions diffuse usually much more slowly than the small ions of the electrolyte (i.e., $D_M \ll D_s$), the coion and counterion concentrations respond quasistatically to the slow dynamics of the macroion density fluctuations described in the reference frame moving at the electrophoretic velocity of the macroions.

(iv) This leads, in particular, to some large length scale perturbations of the local salt concentration $\mathcal{S}$ in the dispersion (i.e., electrodialysis effect), which we have evaluated analytically in two limit regimes. dc limit regime: $L \ll D_s/(L\omega) < \mu_M E_0/\omega$; ac limit regime: $L \gg \max(\mu_M E_0/\omega, \sqrt{D_s/\omega})$, where L is the typical spatial modulation of the macroion fluctuation along the direction of the applied electric field.

(v) Under electric field, this salt perturbation profile is also ''polarized,'' leading to the violation of strict electroneutrality over large length scales in the electrolyte, $\rho_{e_S} = -\varepsilon\varepsilon_0 \vec{E}_0 \cdot \vec{\nabla}\mathcal{S}/2c_s$ (Sec. II).

(vi) The electrical body force arising from the coupling between this large scale charge density and the applied electric field [i.e., $\rho_{e_S}\vec{E}_0$ at first order in c_M/c_s] is then able to trigger some electrohydrodynamic flows in the solution, which can be described in the experimental regimes of interest by a simple Stokes equation in the moving reference frame, $\eta\Delta\vec{v} - \vec{\nabla}P + \rho_{e_S}\vec{E}_0 = \vec{0}$. In particular, $\vec{v}$ has been determined analytically in the Hele-Shaw approximation for a quasi-2D confined geometry (Sec. III).

(vii) The resulting quasistatic electrohydrodynamic flow $\vec{v}$ and the local correction to the applied electric field, $\delta\vec{E}$, are then used to evaluate the slow dynamics of the macroion fluctuations self-consistently [Eq. (4.12) in Sec. IV].

We have numerically solved the self-consistent nonlinear dynamical equation for the macroion fluctuations [Eq. (4.12)] in the Hele-Shaw approximation. This demonstrates the ability of our theoretical model to account for the *dynamic selection process* by which an initially disk-shaped aggregate acquires its eventual quasistationary zigzag structure with tilt angles of $\pm 60°$ in the ac limit regime and $\pm 45°$ in the dc limit regime. In addition, we predict, not only the correct sign of recirculation in the tilted aggregates (similar in both regimes and independent of z_M, the sign of the macroions' charges), but also the correct orders of magnitude for the time scales and recirculation velocities, when experimental values of the various parameters are used.

This good agreement with the experimental observations in both ac and dc limit regimes strongly suggests that the large scale dynamic selection process at work in these various colloidal or polyelectrolyte solutions under strong electric field is indeed related to the nonlinear coupling between the macroion density fluctuations and the associated electrohydrodynamic flows, as discussed in Sec. IV. Moreover, we have suggested that the same nonlinear coupling might also be responsible—through a noise-driven dynamical process—for the primary segregation mechanism itself, as it is shown to dominate the large scale, long time stochastic dynamics in a 3D environment (Appendix B).

Although some important aspects of these segregation and

patterning processes remain to be more thoroughly investigated [30], we believe to have already gained some physical insight into these electrohydrodynamic phenomena. This will have to be further tested through more quantitative experimental studies [31,32]. If confirmed, this understanding should allow improvements of the capillary electrophoresis separation technique. More generally, we expect that the large scale perturbations of ionic distributions in colloidal or polyelectrolyte solutions under electric field should have important consequences in other related problems such as the behavior of electrorheological fluids or the interpretation of dielectric constant measurements in colloidal dispersions [12].

ACKNOWLEDGMENTS

We acknowledge discussions with S. Fraden, J-F. Léger, A. C. Maggs, L. Peliti, M. Seul, and E. Siggia, and thank Y. Hu and L. Mitnik, for discussions and making unpublished data available to us. H.I. would also like to acknowledge the hospitality of the Physics Department of Cornell University, where this work was completed. This work received partial support from the EC grant ''Biomed II Programme'' and the CNRS ''Ultimatech programme.''

APPENDIX A: ELECTROHYDRODYNAMIC FLOW AND OUT-OF-EQUILIBRIUM CHARGE DENSITY

The main contribution to the large scale electrohydrodynamic flow in the macroion dispersion is further discussed in this appendix.

We assume for the sake of simplicity that the primary electrophoretic migration, associated with the counterion equilibrium distribution, does *not* generate any flow in the solution on length scales larger than the Debye length κ^{-1}, as for the case of a ''*free-draining*'' electrophoretic migration [11]. This assumption implies that the large scale electrohydrodynamic flow is related to the out-of-equilibrium charge density. As the salt perturbation profile [Eq. (2.19)] becomes $\mathcal{S}\sim-(\mu_s/\mu_M)c_M$ in the strong field limit $E_0\gg D_s k/\mu_M$, we find, from Eq. (2.20), that the *dynamic* charge density arising from the electrophoretic *migration* of the macroions [i.e., $-\varepsilon\varepsilon_0(\mu_M/\mu_s)\vec{E}_0\cdot\vec{\nabla}c_M/2c_s$] and the charge density associated with the electric polarization of the salt perturbation profile (i.e., $-\varepsilon\varepsilon_0\vec{E}_0\cdot\vec{\nabla}\mathcal{S}/2c_s$) are of similar orders of magnitude (μ_M and μ_s usually having similar numerical values). We expect, however, that the magnitudes of the electrohydrodynamic flow originating from each of these two charge density sources are, in fact, very different. This can been shown by integrating the Stokes equation once over the typical extension length of the flow gradient generated by each of these charge density sources [i.e., $|\vec{\nabla}\vec{v}|\approx(E_0/\eta)\int\rho_e dr_\perp$].

(1) The dynamic charge density originating from the macroions electrophoretic migration generates, in practice, shearing over the Debye length scale κ^{-1}, because of the spatial proximity of the boundary conditions on the actual macroion surface. Its contribution, v_M, to the large scale electrohydrodynamic flow can therefore be estimated as

$$\frac{v_M}{\kappa^{-1}}\approx\varepsilon\varepsilon_0\frac{E_0}{\eta}\left|\int\frac{\mu_M}{\mu_s}\frac{\vec{E}_0\cdot\vec{\nabla}c_M}{2c_s}dr_\perp\right|$$

$$\approx\varepsilon\varepsilon_0\frac{E_0}{\eta}\frac{\mu_M}{\mu_s}\frac{E_0}{2c_s}c_{M_{\max}}.$$

(2) The polarization of the salt perturbation profile $\mathcal{S}$ generates, on the other hand, shearing over the micrometer range scale, which is the typical extension of the salt perturbation in the vicinity of the migrating macroions, i.e., $D_s/(\mu_M E_0)\simeq 1-3\ \mu$m in Eq. (2.19). Hence, the contribution $v_{\mathcal{S}}$ of the salt profile polarization to the large scale electrohydrodynamic flow can be similarly estimated as

$$\frac{v_{\mathcal{S}}}{D_s/(\mu_M E_0)}\approx\varepsilon\varepsilon_0\frac{E_0}{\eta}\left|\int\frac{\vec{E}_0\cdot\vec{\nabla}\mathcal{S}}{2c_s}dr_\perp\right|\approx\varepsilon\varepsilon_0\frac{E_0}{\eta}\frac{E_0}{2c_s}|\mathcal{S}_{\max}|.$$

So using $|\mathcal{S}_{\max}|\approx(\mu_s/\mu_M)c_{M_{\max}}$, from Eq. (2.19) in the strong field limit $E_0\gg D_s k/\mu_M$, we finally get [with $D_s/\mu_M=(\mu_s/\mu_M)kT/e$]

$$v_M\approx\left(\frac{\mu_M}{\mu_s}\right)^3\frac{eE_0\kappa^{-1}}{kT}v_{\mathcal{S}}.$$

Hence we have $v_M\ll v_{\mathcal{S}}$ in most practical situations, suggesting that the contribution to the large scale convection, directly associated with the macroion electrophoretic migration, is generally negligible as compared to the contribution associated with the polarization of the salt perturbation profile far beyond the Debye layers, i.e., $v\approx v_{\mathcal{S}}$. At large length scales, $k^{-1}\gg\kappa^{-1}$, we can therefore simplify the Stokes equation as

$$\eta\Delta\vec{v}-\vec{\nabla}P+\rho_{e_{\mathcal{S}}}\vec{E}_0=\vec{0},$$

with

$$\rho_{e_{\mathcal{S}}}=-\varepsilon\varepsilon_0\vec{E}_0\cdot\vec{\nabla}\mathcal{S}/2c_s.$$

APPENDIX B: RELEVANCE OF NONLINEAR TERMS

We study in this appendix the relevance of the nonlinear terms for the slow dynamics of the macroion density fluctuations starting from the nonlinear dynamical equation (4.12) with the additional (conservative) thermal noise $f(\vec{r},t)$ introduced and discussed in Sec. IV A,

$$d_t\delta\nu_M-D_M\Delta\delta\nu_M+z_M\mu_M\nu_M^0\vec{\nabla}\cdot\delta\vec{E}+z_M\mu_M\vec{\nabla}\cdot(\delta\nu_M\delta\vec{E})$$
$$+\vec{v}\cdot\vec{\nabla}\delta\nu_M+f(\vec{r},t)=0, \tag{B1}$$

with $\langle f(\vec{r},t)f(\vec{r}',t')\rangle\propto\nabla^2\delta^d(\vec{r}-\vec{r}')\delta(t-t')$, where d is the spatial dimension. Investigating for possible dynamic scaling behaviors of Eq. (B1) (as $k\to 0$ and $t\to\infty$), we assume that the change of length scale, $\vec{r}\to b\vec{r}$, is accompanied by the following changes of time scale, $t\to b^z t$, and macroion density fluctuation $\delta\nu_M\to b^\chi\delta\nu_M$, where z is the dynamic exponent that describes the scaling of relaxation times with length, and χ is the analog of the ''roughening exponent'' for a growing interface [19].

We then get the dynamic scaling behaviors of $\delta\vec{E}$ and $\vec{v}$ in Eq. (B1) using Eqs. (4.14) and (4.16) and Eqs. (4.13) and (4.15), respectively. We recall that the (electrohydro)convection given by Eqs. (4.13) and (4.15) is valid only beyond the hydrodynamic screening length a in the Hele-Shaw (HS) approximation (i.e., $k^{-1}>a$). For the sake of generality we will also study the scaling behavior of this term with *no* hydrodynamic screening (NS). One can show that this amounts to simply changing $2/a^2$ into k^2 in Eqs. (4.13) and (4.15). In practice this regime will correspond to length scales smaller than the hydrodynamic screening length, i.e., $k^{-1}<a$. We find the following

(i) In the dc limit regime [from Eqs. (4.13) and (4.14)],

$$\delta E_k^{\mathrm{dc}} \propto \nu_k \quad \text{hence} \quad \delta E^{\mathrm{dc}} \to b^{\chi}\nu_M ,$$

$$v_{\mathrm{HS}_k}^{\mathrm{dc}} \propto k\,\nu_k \quad \text{hence} \quad v_{\mathrm{HS}}^{\mathrm{dc}} \to b^{\chi-1}\nu_M ,$$

$$v_{\mathrm{NS}_k}^{\mathrm{dc}} \propto k^{-1}\nu_k \quad \text{hence} \quad v_{\mathrm{NS}}^{\mathrm{dc}} \to b^{\chi+1}\nu_M .$$

(ii) In the ac limit regime [from Eqs. (4.15) and (4.16)],

$$\delta E_k^{\mathrm{ac}} \propto k\,\nu_k \quad \text{hence} \quad \delta E^{\mathrm{ac}} \to b^{\chi-1}\nu_M ,$$

$$v_{\mathrm{HS}_k}^{\mathrm{ac}} \propto k^3\nu_k \quad \text{hence} \quad v_{\mathrm{HS}}^{\mathrm{ac}} \to b^{\chi-3}\nu_M ,$$

$$v_{\mathrm{NS}_k}^{\mathrm{ac}} \propto k\,\nu_k \quad \text{hence} \quad v_{\mathrm{NS}}^{\mathrm{ac}} \to b^{\chi-1}\nu_M .$$

Assuming that the noise keeps its uncorrelated features under rescaling (as expected at least as long as the nonlinear terms do not dominate) implies the following change of scale for f:

$$f \to b^{-1-d/2-z/2} f .$$

After this rescaling Eq. (B1) transforms to the following:
(i) In the dc limit regime [using Eq. (4.18)],

$$b^{\chi-z} D_t \delta\nu_M - b^{\chi-2} D_M \Delta\,\delta\nu_M + b^{2\chi-1} z_M \mu_M \vec{\nabla}\cdot(\delta\nu_M \delta\vec{E}) + b^{\chi-1+\alpha}\vec{v}\cdot\vec{\nabla}\,\delta\nu_M + b^{-1-d/2-z/2} f(\vec{r},t) = 0,$$

that is,

$$D_t \delta\nu_M - b^{z-2} D_M \Delta\,\delta\nu_M + b^{z-1+\chi} z_M \mu_M \vec{\nabla}\cdot(\delta\nu_M \delta\vec{E}) + b^{z-1+\alpha}\vec{v}\cdot\vec{\nabla}\,\delta\nu_M + b^{-1-d/2+z/2-\chi} f(\vec{r},t) = 0, \tag{B2}$$

where $D_t \equiv [d_t + z_M(\mu_s - \{\mu_M^2/\mu_s\})(N_M \nu_M^0/2c_s)\vec{E}_0\cdot\vec{\nabla}]$ corresponds to the time derivative in the system of reference that moves at uniform velocity, taking into account the corrections in electric field, $z_M\mu_M\vec{E}_0[1+(\{\mu_s/\mu_M\} - \{\mu_M/\mu_s\})(N_M\nu_M^0/2c_s)]$ [see Eq. (4.18)], with $\alpha_{\mathrm{HS}}^{\mathrm{dc}} = \chi - 1$ in the Hele-Shaw approximation and $\alpha_{\mathrm{NS}}^{\mathrm{dc}} = \chi + 1$ on length scales shorter than the electrohydrodynamic screening length.

(ii) In the ac limit regime [using Eq. (4.19)]

$$b^{\chi-z} d_t \delta\nu_M - b^{\chi-2} D_M' \Delta\,\delta\nu_M + b^{2\chi-2} z_M \mu_M \vec{\nabla}\cdot(\delta\nu_M \delta\vec{E}) + b^{\chi-1+\alpha}\vec{v}\cdot\vec{\nabla}\,\delta\nu_M + b^{-1-d/2-z/2} f(\vec{r},t) = 0,$$

that is,

$$d_t \delta\nu_M - b^{z-2} D_M' \Delta\,\delta\nu_M + b^{z-2+\chi} z_M \mu_M \vec{\nabla}\cdot(\delta\nu_M \delta\vec{E}) + b^{z-1+\alpha}\vec{v}\cdot\vec{\nabla}\,\delta\nu_M + b^{-1-d/2+z/2-\chi} f(\vec{r},t) = 0, \tag{B3}$$

where $D_M' = D_M(1+\{N_M\nu_M^0/2c_s\}\{\mu_M kT/eD_M\})$ is an effective diffusion constant taking into account the electric field perturbation effects [see Eq. (4.19)]. With $\alpha_{\mathrm{HS}}^{\mathrm{ac}} = \chi - 3$ in the Hele-Shaw approximation and $\alpha_{\mathrm{NS}}^{\mathrm{ac}} = \chi - 1$ on length scales shorter than the electrohydrodynamic screening length.

In the absence of the nonlinear terms, Eqs. (B2) and (B3) are made scale invariant, as expected, upon the following choices for the dynamic scaling exponents,

$$z = z_0 = 2,$$

$$\chi = \chi_0 = -1 - \frac{d}{2} + \frac{z_0}{2} = -\frac{d}{2}.$$

We then obtain the ''scaling dimension'' of the nonlinear terms, $z_M\mu_M\vec{\nabla}\cdot(\delta\nu_M\delta\vec{E})$ and $\vec{v}\cdot\vec{\nabla}\,\delta\nu_M$, added to this scale-invariant equation, as follows:

(i) In the dc limit regime,

$$z_0 - 1 + \chi_0 = (2-d)/2 \quad \text{for} \quad z_M\mu_M\vec{\nabla}\cdot(\delta\nu_M\delta\vec{E})$$

$$z_0 - 1 + \alpha_0^{\mathrm{dc}} = 1 + \alpha_0^{\mathrm{dc}} \quad \text{for} \quad \vec{v}\cdot\vec{\nabla}\,\delta\nu_M ,$$

with $\alpha_{0\,\mathrm{HS}}^{\mathrm{dc}} = \chi_0 - 1 = -(d+2)/2$ in the Hele-Shaw approximation and $\alpha_{0\,\mathrm{NS}}^{\mathrm{dc}} = \chi_0 + 1 = (2-d)/2$ on length scales shorter than the electrohydrodynamic screening length.

(ii) In the ac limit regime,

$$z_0 - 2 + \chi_0 = -d/2 \quad \text{for} \quad z_M\mu_M\vec{\nabla}\cdot(\delta\nu_M\delta\vec{E}),$$

$$z_0 - 1 + \alpha_0^{\mathrm{ac}} = 1 + \alpha_0^{\mathrm{ac}} \quad \text{for} \quad \vec{v}\cdot\vec{\nabla}\,\delta\nu_M ,$$

with $\alpha_{0\,\mathrm{HS}}^{\mathrm{ac}} = \chi_0 - 3 = -(d+6)/2$ in the Hele-Shaw approximation and $\alpha_{0\,\mathrm{NS}}^{\mathrm{ac}} = \chi_0 - 1 = -(d+2)/2$ on length scales shorter than the electrohydrodynamic screening length.

If the scaling dimensions of both nonlinear terms are *negative*, the nonlinearities scale to zero and are said to be *irrelevant*, so that the solution should remain uniform at large length and time scales as predicted by the linear stability study. [In principle, such situations might also lead to strong coupling regimes for (coupling) parameters exceeding a finite threshold [19,20].] On the other hand, if the scaling dimension of at least one of the nonlinear terms is *positive*, this term grows under rescaling and is *relevant* for the long time, large scale dynamics. Nontrivial dynamic exponents are expected in this case but their estimation through the dynamic renormalization technique is involved [28].

One finally finds for the relevance of the nonlinear terms [25]:

(i) In the dc limit regime, the electrophoretic term $z_M\mu_M\vec{\nabla}\cdot(\delta\nu_M\delta\vec{E})$ is *relevant* for $d\leqslant 2$ [i.e., $(2-d)/2\geqslant 0$] and the convective term $\vec{v}\cdot\vec{\nabla}\delta\nu_M$ is *irrelevant* at any dimension in the Hele-Shaw approximation (i.e., for $k^{-1}>a$ since $-d/2<0$) and *relevant* at $d\leqslant 4$ [i.e., $(4-d)/2\geqslant 0$] on length scales shorter than the hydrodynamic screening length, i.e., $k^{-1}<a$. In particular, in the $d=3$ case, which we are interested in here, we predict that the electrohydrodynamic convective term dominates the long time scale dynamics in the dc limit regime on length scales shorter than the electrohydrodynamic screening length.

(ii) In the ac limit regime, we predict, however, that both nonlinear terms are irrelevant at any dimension or length scales, i.e., $k^{-1}>a$ in the Hele-Shaw approximation and $k^{-1}<a$ for length scales shorter than the electrohydrodynamic screening length.

APPENDIX C: ORDER OF MAGNITUDE OF THE NONLINEAR TERMS

We show in this appendix that the nonlinear electrohydrodynamic convective term, $\vec{v}\cdot\vec{\nabla}\delta\nu_M$, dominates the macroion density fluctuation dynamics (in the moving reference frame) in the conditions of experimental observation with DNA solutions.

In the ac limit regime, we find that this term dominates when the following double inequality holds [we compare, e.g., Eqs. (4.15) and (4.16) and the diffusive term, $D_M k$, with the ac limit constraint, $k^{-1}\gg\mu_M E_0/\omega$],

$$1\ll\frac{\omega^2}{\mu_M^2E_0^2}k^{-2}\ll\frac{3}{32}\frac{\mu_s}{\mu_M}\frac{\varepsilon\varepsilon_0E_0^2a^2}{\eta}\min\left(\frac{c_{M_{\max}}}{2c_sD_M},\frac{e}{kT\mu_M}\right).$$

This typically holds for $k^{-1}\simeq a\simeq 10\ \mu$m, and an electric field of 300 V/cm and 100 Hz in agreement with the experimental conditions for λ-DNA solutions ($\mu_M\simeq 3\times10^{-8}\ \mathrm{m^2\,V^{-1}\,s^{-1}}$, $\mu_s\simeq10^{-7}\ \mathrm{m^2\,V^{-1}\,s^{-1}}$, $D_M\simeq10^{-12}\ \mathrm{m^2\,s^{-1}}$, $c_{M_{\max}}/2c_s\simeq10^{-2}$, $\eta\simeq10^{-3}$ Pa s, and $\varepsilon\varepsilon_0\simeq10^{-9}\ \mathrm{F\,m^{-1}}$).

In the dc limit regime, i.e., $k^{-1}\ll D_sk/\omega<\mu_ME_0/\omega$, we find similarly that the electrohydrodynamic convective term dominates the dynamics when the following two inequalities hold [we compare, e.g., Eqs. (4.13) and (4.14) and the diffusive term, D_Mk],

$$k^{-1}\ll\varepsilon\varepsilon_0E_0\frac{a^2}{2\eta}\frac{\mu_s^2}{\mu_M(\mu_s^2-\mu_M^2)},$$

$$D_M\ll\frac{\mu_s}{\mu_M}\frac{\varepsilon\varepsilon_0E_0^2a^2}{\eta}\frac{c_{M_{\max}}}{4c_s}.$$

This also typically holds in the experimental conditions with the λ-DNA solutions.

[1] L. Mitnik, C. Heller, J. Prost, and J-L. Viovy, Science **267**, 219 (1995).

[2] L. Mitnik, thèse de l'Université de Paris 6 (1995).

[3] *Capillary Electrophoresis: An Analytical Tool in Biotechnology*, edited by P. G. Righetti (CRC Press, Boca Raton, FL, 1996).

[4] H. Isambert, A. Ajdari, J-L. Viovy, and J. Prost, Phys. Rev. Lett. **78**, 971 (1997).

[5] Y. Hu, J. L. Glass, A. E. Griffith, and S. Fraden, J. Chem. Phys. **100**, 4674 (1994).

[6] B. R. Jennings and M. Stankiewicz, Proc. R. Soc. London, Ser. A **427**, 321 (1990).

[7] D. Stigter, J. Chem. Phys. **82**, 1417 (1978); **82**, 1424 (1978).

[8] M. von Smoluchowski, Bull. Int. l'Acad. Sci. Cracovie **8**, 182 (1903).

[9] See, e.g., R. J. Hunter, *Foundations of Colloid Science*, Vol. 2 (Clarendon Press, Oxford, 1989); or W. B. Russel, D. A. Saville, and W. R. Schowalter, *Colloidal Dispersions* (Cambridge University Press, Cambridge, 1989).

[10] T. C. Halsey and W. Toor, Phys. Rev. Lett. **65**, 2820 (1990).

[11] G. S. Manning, J. Phys. Chem. **85**, 1506 (1981).

[12] Although the present work merely applies for colloidal dispersions of high ionic strength, i.e., $c_{M_{\max}}/c_s\ll1$, the electrohydrodynamic effects we predict become enhanced at lower ionic strength, that is as $c_{M_{\max}}/c_s\to1$. Furthermore this suggests that the usual assumption of small perturbations beyond the Debye layers might well be jeopardized in many practical situations as, e.g., for the dielectric constant measurements of colloidal dispersions.

[13] In fact different diffusion constants of the coions and counterions (i.e., $D_+\neq D_-$) do *not* change the main conclusions of our paper as one can show that the leading part of the out-of-equilibrium charge density in the solution surrounding the macroions, ρ_{e_S}, does *not* depend upon these diffusion constants. Namely,

$$\rho_{e_S}=\frac{\varepsilon\varepsilon_0}{2c_s}\left[\left(\frac{D_+-D_-}{D_++D_-}\right)\frac{kT}{e}\Delta\mathcal{S}-\vec{E}_0.\vec{\nabla}\mathcal{S}\right]\sim-\frac{\varepsilon\varepsilon_0}{2c_s}\vec{E}_0\cdot\vec{\nabla}\mathcal{S}$$

under the strong electric field condition, $eE_0\diagup/kT\gg1$.

[14] G. K. Batchelor, *An Introduction to Fluid Dynamics* (Cambridge University Press, Cambridge, 1967).

[15] More precisely, this result of the classical theory [9] is related to the *a priori* assumption of stationarity, which eliminates the transient regimes and therefore prevents detection of the dynamical instabilities of the ionic distributions under the application of any finite electric field.

[16] This can be shown, e.g., using the same formalism developed in Sec. II to describe the salt profile in the frame of reference moving at the velocity $\dot{\vec{r}}_0=z_M\mu_M\vec{E}_0$. With the hydrodynamic flow described in this ''transported'' frame of reference—i.e., $\vec{v}\equiv\vec{v}(\vec{r}-\vec{r}_0(t),t)$—the linearized Navier-Stokes equation becomes (see Appendix A for justification of the term $\rho_{e_S}\vec{E}_0$)

$$\rho(\partial_t\vec{v}-z_M\mu_M(\vec{E}_0.\vec{\nabla})\vec{v})+\eta\Delta\vec{v}-\vec{\nabla}P+\rho_{e_S}\vec{E}_0=\vec{0},$$

which simplifies at low frequency, $\omega\ll\eta/(\rho L^2)$, to the usual

Stokes equation if the vorticity diffuses faster than the electrophoretic motion over the typical width, L, of the macroion aggregates, i.e., $\eta/(\rho L^2) \gg \mu_M E_0/L$.

[17] This result implies in fact that the double inequality $1 \gg \mu_M \vec{E}_0 \cdot \vec{k}/\omega \gg c_{M_{\max}}/c_s$ holds so that the nonlinear corrections of order $O((c_{M_{\max}}/c_s)^2)$ are indeed negligible in Eqs. (2.15), (3.10), and (3.11) as compared to those of order $O((c_{M_{\max}}/c_s)(\mu_M \vec{E}_0 \cdot \vec{k}/\omega))$ in Eqs. (3.9), (3.10), and (3.11).

[18] H. Isambert (unpublished). Constant electrophoretic mobilities and diffusion constants have been assumed [27].

[19] M. Kardar, G. Parisi, and Y. C. Zhang, Phys. Rev. Lett. **56**, 889 (1986).

[20] *Scale Invariance, Interfaces, and Non-Equilibrium Dynamics*, edited by A. McKane, M. Droz, J. Vannimenus, and D. Wolf (Plenum Press, New York, 1995); and A.-L. Barabási and H. E. Stanley, *Fractal Concepts in Surface Growth* (Cambridge University Press, Cambridge, 1995).

[21] D. Foster, D. R. Nelson, and M. J. Stephen, Phys. Rev. A **6**, 732 (1977).

[22] H. Mori, Prog. Theor. Phys. **53**, 1617 (1975).

[23] N. G. van Kampen, *Stochastic Process in Physics and Chemistry* (North-Holland, Amsterdam, 1981), Chap. 8.

[24] K. M. van Vliet, J. Math. Phys. (N.Y.) **12**, 1981 (1971); **12**, 1998 (1971).

[25] Note that the *local* stochastic PDE usually studied in the literature in relation to dynamic scaling behaviors [20] *cannot* lead to the relevance of their nonlinear terms at $d=3$ with a *conservative* noise source obeying $\langle f(\vec{r},t) f(\vec{r}',t') \rangle \propto \nabla^2 \delta^d(\vec{r}-\vec{r}') \delta(t-t')$. This is the reason why the conservative random noise arising as a result of the derivation of the Navier-Stokes equation from the microscopic equations of motion can safely be neglected in hydrodynamic calculations above two dimensions [26]. In contrast, the relevant nonlinear coupling between the (macroion) density fluctuations and the associated electrohydrodynamic flow that we have exhibited in this conservative system, is *nonlocal* (see, e.g., $v^{\mathrm{dc}}_{NS_k} \propto k^{-1} \nu_k$ in Appendix B).

[26] D. Foster, D. R. Nelson, and M. J. Stephen, Phys. Rev. Lett. **36**, 867 (1976); V. Yakhot and Z.-S. She, J. Math. Phys. (N.Y.) **60**, 1840 (1988).

[27] Although we can imagine other more traditional instabilities to occur from the purely deterministic dynamical equations if we consider, for instance, the possibility of variation of the electrophoretic mobilities (e.g., $\partial\mu/\partial E_0 < 0$), such mechanisms cannot explain, however, the experimentally observed differences between hydrodynamically screened and unscreened length scales as they do not involve hydrodynamics.

[28] In addition to the already mentioned changes of stochastic properties of the internal noise under dynamic rescaling, a quantitative study should also allow the *ab initio* possibility of spatially anisotropic scalings in reference to the observed dynamical patterns with broken symmetry. Such a requirement leads to the unfortunate consequence of multiplying the number of coupling parameters that transform differently under rescaling, and seems to prevent further analytical progress with reasonable calculation work.

[29] W. H. Press, S. A. Teukolsky, W. T. Veterling, and B. P. Flannery, *Numerical Recipes*, 2nd ed. (Cambridge University Press, Cambridge, 1992).

[30] Of particular interest is the long time scale evolution (typically longer than about 10 min) of the quasi-2D patterns, which is controlled by the rare and sudden mergings of the quasistationary dynamical tilted aggregates to form longer—and somewhat wider—ones with progressively larger angle of tilt with respect to the field as experimentally reported in [6].

[31] S. Magnúdóttir *et al.* (unpublished).

[32] B. Ladoux *et al.* (unpublished).